Energy-Efficient Timely Transportation of Long-Haul Heavy-Duty Trucks

Lei Deng, Mohammad H. Hajiesmaili, Minghua Chen, *Senior Member, IEEE,* and Haibo Zeng, *Member, IEEE*

Abstract—We consider a timely transportation problem where a heavy-duty truck travels between two locations across the national highway system, subject to a hard deadline constraint. Our objective is to minimize the total fuel consumption of the truck, by optimizing both route planning and speed planning. The problem is important for cost-effective and environment-friendly truck operation, and it is uniquely challenging due to its combinatorial nature as well as the need of considering hard deadline constraint. We first show that the problem is NP-Complete; thus exact solution is computational prohibited unless P=NP. We then design a fully polynomial time approximation scheme (FPTAS) to solve it. While achieving highly-preferred theoretical performance guarantee, the proposed FPTAS still suffers from long running time when applying to national-wide highway systems with tens of thousands of nodes and edges. Leveraging elegant insights from studying the dual of the original problem, we design a heuristic with much lower complexity. The proposed heuristic allows us to tackle the energy-efficient timely transportation problem on large-scale national highway systems. We further characterize a condition under which our heuristic generates an optimal solution. We observe that the condition holds in most of practical instances in numerical experiments, justifying the superior empirical performance of our heuristic. We carry out extensive numerical experiments using real-world truck data over the actual U.S. highway network. The results show that our proposed solutions achieve 17% (resp. 14%) fuel consumption reduction, as compared to a fastest path (resp. shortest path) algorithm adapted from common practice.

Index Terms—Energy-efficient transportation, timely delivery, route planning, speed planning.

I. INTRODUCTION

In the U.S., heavy-duty trucks haul more than 70% of all freight tonnage [2], and they consume 17.6% of energy in transportation sector [3, Tab. 2.8] and contribute to about 5% of the greenhouse gas emission [4]. Fuel cost is the largest operating cost (34%) of truck owners/operators [5], and reducing fuel consumption is critical for cost-effective and environment-friendly heavy-duty truck operations.

Currently there are mainly two lines of efforts to reduce fuel consumption of heavy-duty trucks. The first line is to operate with more fuel efficient trucks, from better designs for engines, drivetrains, aerodynamics, and tires [6]–[8], to better management of truck parts such as maintaining optimal tire pressures [9]. The second line is to operate heavy-duty trucks more economically. This explores several possibilities, e.g., reducing idling energy consumption [10], platooning more than one heavy-duty trucks [11], [12], route planning [13]–[15], and speed planning [16]–[19]. In this paper, we focus on route and speed planning. Different routes could have different mileages, levels of congestion, road grades, and surface types, etc., all of which would largely affect the fuel consumption. Real-world studies [15] show that choosing a more efficient route for a heavy-duty truck can improve its fuel economy by 21%. Speed planning is another well recognized approach to effectively reduce fuel consumption. Different running speed could lead to different fuel economy. For a vehicle with certain weight running on a road, normally there is a most fuel-efficient speed. When the running speed is below or above the most fuel-efficient speed, the fuel economy will be degraded. As a rule of thumb for truck operations on highway, every one mile per hour (mph) increase in speed (above the most fuel-efficient speed) incurs about 0.14 mile per gallon (mpg) decrease in fuel economy [18], [19].

However, operating at low speed may result in excessive travel time and the goods carried by the truck cannot be delivered on time. We remark that timely delivery is critical for truck operators [20], [21]. As estimated by the U.S. Federal Highway Administration (FHWA) in [20], unexpected delay can increase freight cost by 50% to 250%. Multiple reasons can explain the importance of timely delivery. First, some freight goods are perishable, such as food [22], which definitely require timely delivery. Second, to ensure customers' satisfaction, some companies, e.g., Amazon, may have a service-level agreement (SLA) with users, under which the delivery delay is guaranteed [23]. Finally, violating scheduled delay can introduce difficulties for global logistic decisions and even increase the uncertainty and inefficiency of supply chains [20]. Overall, it is crucial to ensure timely goods delivery for truck operators, and considering timely delivery in fuel cost minimization poses a unique challenge.

Motivated by the above observations, in this paper, we study the problem of *energy-efficient timely transportation* for heavy-duty trucks. We aim to minimize the heavy duty truck's fuel consumption while satisfying a hard deadline constraint, under which we take both route planning and speed planning into account to exploit complete design space of reducing

TABLE I
COMPARISONS OF OUR STUDY AND EXISTING WORKS ON PERFORMANCE OPTIMIZATION IN VARIOUS TRANSPORTATION SYSTEMS WITH DELAY TAKEN
INTO CONSIDERATION. HERE RSP STANDS FOR RESTRICTED SHORTEST PATH PROBLEM, VRPTW STANDS FOR VEHICLE ROUTING PROBLEM WITH
TIME WINDOWS, AND BSP STANDS FOR BI-OBJECTIVE SHORTEST PATH PROBLEM.

		Our Work	**RSP** [24]–[26]	**VRPTW** [27]–[30]	**Other Works** [31], [32]	**BSP** [33]–[36]
Settings	Objective	Cost minimization	Cost minimization	Cost minimization	Cost minimization or profit maximization	Bi-objective (cost and delay) minimization
	Constraints	A hard deadline	A hard deadline	Time window⋆, Other constraints	Time window⋆, Other constraints	N/A
	Design Spaces	Route planning, Speed planning	Route planning	Route planning	Route planning, Speed planning	Route planning
Results	Hardness	NP-Complete	NP-Complete [25]	NP-Complete [27]	N/A	NP-Complete [33]
	Algorithms	FPTAS, Heuristic†	FPTAS [24], Heuristic [26]	Heuristic [28]–[30]	Heuristic	FPTAS [34], [35], Heuristic [36]

⋆ The time window constraint captures the hard deadline constraint in our problem and RSP as a special case.
† We further characterize a condition under which the heuristic outputs the optimal solution to our problem.

TABLE II
COMPARISONS OF OUR WORK AND EXISTING WORKS ON
ENERGY-EFFICIENT HEAVY-DUTY TRUCK OPERATION.

Paper	Route Planning	Speed Planning	Hard Deadline
[37]	✓	✗	✗
[16]	✗	✓	✗
[17]	✗	✓	✓
This work	✓	✓	✓

fuel consumption. Since heavy-duty trucks are mainly operated for *long-haul* delivery and most of time run on highways [3, Tab. 5.2 and Fig. 5.1], we focus our model on their operation in the highway transportation network system. We summarize our contributions in the following.

▷ We formulate an energy-efficient timely transportation problem of minimizing the fuel consumption subject to a hard deadline constraint for a heavy-duty truck running on a highway transportation network, with design spaces of both route planning and speed planning in Sec. II. To the best of our knowledge, as compared to existing works on energy-efficient heavy-duty truck operation [16], [17], [37], our work is the first one that simultaneously considers route planning, speed planning, and hard deadline (see Tab. II).

▷ We show that our problem is NP-Complete and then design a fully polynomial time approximation scheme (FPTAS) in Sec. III to solve our problem. The proposed FPTAS attains an approximation ratio of $(1 + \epsilon)$ with a network-size induced complexity of $O(mn^2/\epsilon^2)$, where m and n are the numbers of nodes and edges, respectively.

▷ While achieving highly-preferred theoretical performance guarantee, the proposed FPTAS still suffers from long running time when applying to national-wide highway systems with tens of thousands of nodes and edges. In Sec. IV, by leveraging elegant insights from studying the dual of the original problem, we design a fast heuristic solution with $O(m + n \log n)$ complexity. The proposed heuristic scheme allows us to tackle the energy-efficient timely transportation problem on large-scale national highway systems. We further characterize a condition under which our heuristic generates an optimal solution. We observe that the condition holds in most of

the practical instances in numerical experiments in Sec. V, justifying the superior empirical performance of our heuristic.

▷ We carry out extensive numerical experiments using real-world truck data over the U.S. highway network in Sec. V. The results show that our proposed solutions achieve 17% (resp. 14%) fuel consumption reduction, as compared to a fastest path (resp. shortest path) algorithm adapted from common practice. The amount of fuel consumption saving is enough to power up more than 90% of the entire transportation sector in New York State [38].

Comparison with existing works on energy-efficient heavy-duty truck operation. There are a large number of works focusing on energy-efficient heavy-duty truck operation, e.g., [16], [17], [37]. But to the best of our knowledge, our work is the first one that simultaneously considers route planning, speed planning, and hard deadline (see Tab. II).

Comparison with existing works on performance optimization in various transportation systems with delay taken into consideration. Theoretically, we also compare the problem studied in our work with other related problems studied in existing works in Tab. I. First, our energy-efficient timely transportation problem is a generalized version of Restricted Shortest Path problem (RSP) [24]–[26], with an extra design space of speed planning. Therefore, we generalize the FPTAS design and the dual-based design of RSP to our problem. Second, for the well-studied Vehicle Routing Problem with Time Windows (VRPTW) [27]–[30], if we only consider one vehicle and one customer with departure deadline, then it becomes the RSP problem, which is a special case of our problem without speed planning. Third, our problem can be regarded as a special case of the studied problems in [31], [32] under different contexts from our focus on trucks, where both route planning and speed planning are considered. However, [31], [32] do not prove the hardness of the problem and only propose a heuristic algorithm without performance guarantee to solve the problem. The heuristic algorithm in [31] uses the column generation approach but terminates in certain iterations, and the heuristic algorithm in [32] is based on a multi-start local search approach, both of which could incur high complexity and do not have performance guarantee. The performance of these generic approaches can be quite
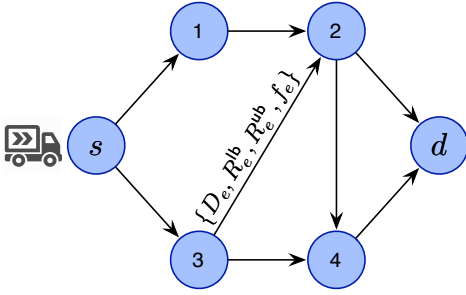
Fig. 1. System model.

unsatisfactory in some specific problems. For example, column generation approach suffers from slow convergence and thus terminating in certain iterations could produce a solution far away from the optimal one [39], [40], and multi-start local search could also get trapped in a bad local optimum [41]. Our work, instead, shows that our studied problem is NP-complete, and proposes an FPTAS and a heuristic algorithm with characterizing an optimality condition to solve the problem. Our numeric results in Sec. V demonstrate the excellent performance of our solutions in practical scenarios. We also explicitly show that the time complexity of the FPTAS and the heuristic is polynomial in the problem size. Finally, another related problem is the Bi-objective Shortest Path problem (BSP) [33]–[36], which needs to find all Pareto-optimal paths to simultaneously minimize the travel cost and travel time. BSP is different from our problem in that it regards the travel time as one objective instead of a constraint to satisfy and it does not have the design space of speed planning.

Due to the space limitation, all proofs are included in the supplementary materials.

II. MODEL AND PROBLEM FORMULATION

A. System Model

Consider a highway transportation network as exemplified in Fig. 1. We model it as a directed graph $\mathcal{G} = (\mathcal{V}, \mathcal{E})$, where $\mathcal{V}$ is the vertex/node set and $\mathcal{E}$ is the edge/road set. We define $n \triangleq |\mathcal{V}|$ as the number of nodes and $m \triangleq |\mathcal{E}|$ as the number of edges. For each edge $e \in \mathcal{E}$, we denote $D_e > 0$ as its distance (unit: mile), and $R_e^{\text{lb}} > 0$ (resp. $R_e^{\text{ub}} \geq R_e^{\text{lb}}$) as its minimum (resp. maximum) speed (unit: mph). (Governments usually set the maximum speed for all highways and the minimum speed for some highways. For the sake of both safety and fuel efficiency, lower speed limits than passenger cars may be applied to large commercial vehicles like heavy-duty trucks and buses.) Now consider a long-haul heavy-duty truck at time 0 who aims to ship cargos from a source node $s \in \mathcal{V}$ to a destination node $d \in \mathcal{V}$. The goal is to minimize the energy/fuel[1] consumption subject to a *hard* deadline requirement $T > 0$ (unit: hour).

Fuel consumption and travel delay are usually in conflict with each other, both of which are related to the speed profile of the truck. High travel speed obviously decreases the travel delay, but it can also increase the fuel consumption

[1]We interchangeably use *fuel* and *energy* in this paper.

significantly [18], [19]. To analyze the performance tradeoff between energy and delay, we need to model the relationship between the fuel consumption and the travel speed. There are an intensive number of such models (see a survey in [42]). In this paper, we use the instantaneous fuel consumption model [42], [43] which generally depends on three factors: (i) static vehicle/road/environment properties, (ii) instantaneous acceleration/deceleration, and (iii) instantaneous speed. As we consider a specific vehicle running over a specific network, static vehicle/road/environment properties are fixed, and thus we model them as fixed parameters in our fuel consumption model. We further neglect the effects of instantaneous acceleration/deceleration based on the following two observations. First, as shown in [44], [45] and our results in Lemma 1, running at a constant speed is most fuel-economic on a road segment with homogeneous grade and road/environment conditions. Thus, it is reasonable to ignore the effects of acceleration/deceleration inside any road segment (with homogeneous grade and road/environment conditions). Second, while a truck may involve acceleration/deceleration when switching from one road segment to another road segment, the acceleration/deceleration distance is negligible as compared to the length of road segments. For example, as shown in [46], the heavy-duty truck can accelerate from zero speed to 31mph in just 500 feet, while the average length of highway road segments is 3.26 miles, according to our study of the U.S. national highway data (see Tab. IV). Thus, it is also reasonable to ignore the effects of acceleration/deceleration during road segment switch. With the above justification, in this paper, we assume that the instantaneous fuel consumption is a function of the instantaneous speed.

We thus define $f_e : [R_e^{\text{lb}}, R_e^{\text{ub}}] \to \mathbb{R}^+$ as the (instantaneous) *fuel-rate-speed function* of the truck running on edge e: if the vehicle's speed on edge e is r_e (unit: mph), the fuel consumption rate is $f_e(r_e)$ (unit: gallons per hour (gph)), and then the total fuel consumption for driving time τ (unit: hour) with the constant speed r_e is $f_e(r_e) \cdot \tau$ (unit: gallon). Since many existing models [43], [47]–[50] use polynomial functions to model the fuel consumption which are also strictly convex in a reasonable speed limit region, in this paper, we assume that $f_e(\cdot)$ is a polynomial function and is strictly convex[2] over $[R_e^{\text{lb}}, R_e^{\text{ub}}]$. This assumption also holds in the physical interpretation of fuel-rate-speed function as shown in Append. A in the supplementary materials, and is further verified in our simulation using real-world data (see Fig. 5(a)).

B. Problem Formulation

We consider two design spaces: path selection (route planning) and speed optimization (speed planning). For path selection, we define a binary variable x_e for any $e \in \mathcal{E}$,

$$x_e = \begin{cases} 1, & \text{Edge } e \text{ is on the selected path;} \\ 0, & \text{otherwise.} \end{cases} \quad (1)$$

For the speed optimization, the truck needs to determine a speed profile (speeds at all travel time) over any selected

[2]The strict convexity can be relaxed to convexity. For simplicity, we use the strict convexity in this paper.

edge. This is a functional variable, but the convexity of fuel-rate-speed function can simplify the speed profile significantly based on the following lemma.

Lemma 1: For any edge e, if the travel time t_e is given, i.e., the truck must pass edge e with exactly t_e hours, then the optimal speed profile to minimize the fuel consumption is to maintain constant speed D_e/t_e during the whole trip.

Proof: See Append. B in the supplementary materials. ∎

Lemma 1 shows that for any edge, any non-constant speed profile is dominated by another constant speed profile in terms of fuel consumption without sacrificing the delay performance. Therefore, without loss of optimality, the truck only needs to follow a constant speed for any edge. As explained in Sec. II-A, since we consider a long-haul highway scenario, we will ignore the speed transition period between two adjacent edges. Thus, for the speed optimization, we consider the travel time $t_e > 0$ over each edge e as the design variable, which equivalently implies a constant speed D_e/t_e over e. We then define a *fuel-time* function $c_e(\cdot)$ for each road e,

$$c_e(t_e) \triangleq t_e \cdot f_e(\frac{D_e}{t_e}), \tag{2}$$

which is the total fuel consumption for the truck traveling edge e with travel time t_e.

By vectorizing our decision variables as $\boldsymbol{x} \triangleq \{x_e : e \in \mathcal{E}\}$ and $\boldsymbol{t} \triangleq \{t_e : e \in \mathcal{E}\}$, now we are ready to formulate our PAth selection and Speed Optimization (PASO) problem,

$$\text{PASO:} \min_{\boldsymbol{x} \in \mathcal{X}, \boldsymbol{t} \in \mathcal{T}} \quad \sum_{e \in \mathcal{E}} x_e \cdot c_e(t_e) \tag{3}$$

$$\text{s.t.} \quad \sum_{e \in \mathcal{E}} x_e t_e \leq T, \tag{4}$$

In PASO, set $\mathcal{X}$ restricts that one and only one $s - d$ path is selected, defined as

$$\mathcal{X} \triangleq \{\boldsymbol{x} : x_e \in \{0, 1\}, \forall e \in \mathcal{E}, \text{ and}$$
$$\sum_{e \in \mathsf{out}(v)} x_e - \sum_{e \in \mathsf{in}(v)} x_e = 1_{\{v=s\}} - 1_{\{v=d\}}, \forall v \in \mathcal{V}\},$$

where $1_{\{\cdot\}}$ is the indicator function, $\mathsf{in}(v) \triangleq \{(u, v) : (u, v) \in \mathcal{E}\}$ is the set of incoming edges of node $v \in \mathcal{V}$, $\mathsf{out}(v) \triangleq \{(v, u) : (v, u) \in \mathcal{E}\}$ is the set of outgoing edges of node v. Set $\mathcal{T}$ captures the speed limits of all roads, defined as

$$\mathcal{T} \triangleq \{\boldsymbol{t} : t_e^{\mathsf{lb}} \leq t_e \leq t_e^{\mathsf{ub}}, \forall e \in \mathcal{E}\},$$

where $t_e^{\mathsf{lb}} \triangleq \frac{D_e}{R_e^{\mathsf{ub}}}$ and $t_e^{\mathsf{ub}} \triangleq \frac{D_e}{R_e^{\mathsf{lb}}}$ are the minimum and maximum travel time due to the speed limits on edge e, respectively. Constraint (4) is to satisfy the hard deadline requirement. Objective (3) is to minimize the total fuel consumption over the selected path.

Note that one major difficulty of our problem PASO is that the route planning and the speed planning are coupled with each other and thus we need to tackle them simultaneously.

C. Complexity Hardness

PASO has both integer variables and continuous variables. Thus it is worth understanding its hardness first. It turns out that a special case of PASO is the well-known Restricted

Shortest Path (RSP) problem [24], [25]. In RSP, a directed graph is given where each edge has a *fixed* travel time and travel cost, and the goal is to find a minimum-cost path subject to a hard path deadline requirement. Clearly, our problem PASO generalizes RSP where we allow a varying edge cost and edge time because of the design space of speed optimization. Since RSP is NP-Complete [25], we can thus easily prove that our problem PASO is also NP-Complete.

Theorem 1: PASO is NP-Complete.

Proof: We can prove it by setting $R_e^{\mathsf{lb}} = R_e^{\mathsf{ub}}$ to an appropriate value for each edge e in PASO, and using the result that RSP is NP-Complete [25]. ∎

Theorem 1 shows that exact solution is computational prohibited unless P=NP. In this paper, we thus seek approximate but efficient solutions to PASO.

D. Preprocessing and Some Notations

We first check the feasibility of our problem PASO. We can use the shortest path algorithm where each edge e has cost t_e^{lb} to find the fastest path. If the travel time of the fastest path is larger than the deadline requirement T, PASO is infeasible. In the rest of this paper, we thus assume that the deadline constraint T is at least the travel time of the fastest path such that the problem is feasible.

We then analyze properties of the fuel-time function $c_e(\cdot)$.

Lemma 2: $c_e(t_e)$ is strictly convex over $[t_e^{\mathsf{lb}}, t_e^{\mathsf{ub}}]$. Also, there exists a point $\hat{t}_e \in [t_e^{\mathsf{lb}}, t_e^{\mathsf{ub}}]^3$ such that $c_e(t_e)$ is first strictly decreasing over $[t_e^{\mathsf{lb}}, \hat{t}_e]$ and then strictly increasing over $[\hat{t}_e, t_e^{\mathsf{ub}}]$.

Proof: See Append. C in the supplementary materials. ∎

Based on Lemma 2, we can easily prove that the travel time over edge e, i.e., t_e, in any optimal solution of PASO must be in the region $[t_e^{\mathsf{lb}}, \hat{t}_e]$. Otherwise, we can decrease the travel time from t_e to $\hat{t}_e$ and at the same time decrease the fuel consumption, which violates the optimality of t_e. Thus, without loss of optimality, we can reset the travel time limit from $[t_e^{\mathsf{lb}}, t_e^{\mathsf{ub}}]$ to $[t_e^{\mathsf{lb}}, \hat{t}_e]$, which equivalently implies that we reset the speed limit from $[R_e^{\mathsf{lb}}, R_e^{\mathsf{ub}}]$ to $[D_e/\hat{t}_e, R_e^{\mathsf{ub}}]$. After such preprocessing, in the rest of the paper, $c_e(t_e)$ can be assumed to be *strictly convex and strictly decreasing* over $t_e \in [t_e^{\mathsf{lb}}, t_e^{\mathsf{ub}}]$ *without loss of optimality*.

In the rest of the paper, define an $s - d$ path p as the set of all *edges* over p and $\boldsymbol{t}_p \triangleq \{t_e : e \in p\}$ as the corresponding travel time set. Moreover, we define $c(p, \boldsymbol{t}_p) \triangleq \sum_{e \in p} c_e(t_e)$ as the fuel consumption of path p with travel time set $\boldsymbol{t}_p$, and OPT as the optimal value of PASO.

Next, we will propose a fully polynomial time approximation scheme (FPTAS) in Sec. III and a fast dual-based heuristic scheme in Sec. IV to solve our problem PASO.

III. AN FPTAS FOR PASO

Since PASO generalizes RSP, which is well-known to have an FPTAS [24], [51], it is natural to ask whether we can extend RSP's FPTAS for our problem PASO. In this section, by carefully tackling the difference between PASO and RSP, we

---

³Note that $\hat{t}_e$ can be on the boundary.

"reformulate" PASO such that we can adapt RSP's FPTAS to construct an FPTAS for PASO. More specifically, in this section, we propose an approximation scheme (Algorithm 3) such that for any given $\epsilon \in (0,1)$, it can find a $(1+\epsilon)$-approximate solution in the sense that the solution is *feasible* and the corresponding fuel consumption is at most $(1+\epsilon)$OPT, and the time complexity is polynomial in both the problem size and $\frac{1}{\epsilon}$.

The essence of RSP's FPTAS [24], [51] is a test procedure. For any input value $S > 0$ and any input accuracy parameter $\delta > 0$, the test procedure can "approximately" compare S and the optimal value OPT in the sense that it can tell either OPT $> S$ or OPT $\leq (1+\delta)S$ in polynomial time. Based on this test procedure, starting with some arbitrary lower bound LB and upper bound UB for OPT, a binary search scheme is designed [24], [51] to exponentially narrow down the bounding interval [LB, UB] and finally a $(1+\epsilon)$-approximate solution is outputted.

To solve our problem PASO, we adapt RSP's FPTAS by designing our own test procedure. In RSP, [24] and [51] use the *rounding and scaling* technique, where each *fixed* edge cost is rounded into certain (polynomial) number of cost levels controlled by the accuracy parameter δ. As we only require an "approximate" comparison, rounding into certain number of cost levels is enough to perform such a task. However, as opposed to a fixed edge cost in RSP, in PASO each edge has a fuel-time function. Hence, instead of rounding a fixed cost in RSP, we *quantize* the continuous fuel-time function $c_e(\cdot)$ into another staircase fuel-time function $\tilde{c}_e(\cdot)$ according to the input value S and the input accuracy parameter δ, which can be further characterized by a polynomial number of *representative points*. We then prove that such quantization can perform the "approximate" comparison.

Later on we will describe our algorithms in a bottom-up fashion. We first describe the quantizing procedure (Algorithm 1) in Sec. III-A. Then we present our own test procedure (Algorithm 2) which invokes Algorithm 1 in Sec. III-B. Finally, we describe the whole FPTAS (Algorithm 3) which invokes Algorithm 2 in Sec. III-C.

A. Quantizing Fuel-Time Function

For any input value $V > 0$ and $N \in \mathbb{Z}^+$, we quantize the edge-e fuel-time function $c_e(t_e)$ to be

$$\tilde{c}_e(t_e) \triangleq \min\left\{\left\lfloor \frac{c_e(t_e)}{V} \right\rfloor + 1, N\right\}, \forall t_e \in [t_e^{\text{lb}}, t_e^{\text{ub}}]. \quad (5)$$

Since we have assumed that $c_e(t_e)$ is strictly decreasing in Sec. II-D, $\tilde{c}_e(t_e)$ thus becomes a *staircase* function with at most N stairs. During the quantization, parameter V is to control the accuracy, which is the vertical span of each stair. Larger V means rougher quantization and lower accuracy but smaller complexity. Parameter N is to control the maximum number of stairs. Since $c_e(t_e)$ could take an arbitrarily large value, the number of stairs could be unbounded, which definitely incurs high complexity. To design a polynomial time test procedure where we only need to perform an "approximate" comparison, we truncate $c_e(t_e)$ by putting a ceil VN. This
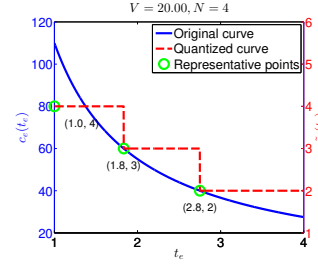

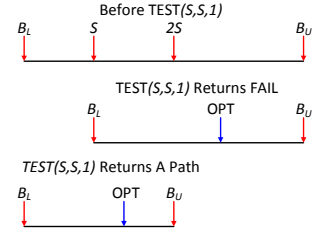Fig. 2. An example for quantizing $c_e(\cdot)$.

Fig. 3. Binary search (*Step 2*) of Algorithm 3.

truncation is sufficient for use in the test procedure (see Sec. III-B). Clearly, $\tilde{c}_e(t_e)$ is a *quantized and truncated* version of $c_e(t_e)$. An example is shown in Fig. 2. Here we set $V = 20, N = 4$. Thus, each stair spans 20 and $c_e(t_e)$ is truncated by the ceil $VN = 80$. The resulting curve $\tilde{c}_e(t_e)$ is a non-increasing staircase function, which jumps from 4 to 3 at $t_e = 1.8$ and jumps from 3 to 2 at $t_e = 2.8$.

Moreover, since $\tilde{c}_e(t_e)$ is a staircase function and only takes integer values, we can use an N-dim vector $\boldsymbol{\tau}_e$ to represent it without any information loss. We define it as $\boldsymbol{\tau}_e \triangleq (\tau_e^1, \tau_e^2, \cdots, \tau_e^N)$ where τ_e^i is the minimum travel time over $[t_e^{\text{lb}}, t_e^{\text{ub}}]$ such that $\tilde{c}_e(\cdot) = i$ and is defined as nan if $\tilde{c}_e(\cdot) = i$ has no solution. For the example in Fig. 2, we have $\tau_e = (\tau_e^1, \tau_e^2, \tau_e^3, \tau_e^4) = (\text{nan}, 2.8, 1.8, 1)$.

We call (τ_e^i, i) the i-th *representative point* of $\tilde{c}_e(\cdot)$. Thus $\tilde{c}_e(\cdot)$ is characterized by at most N representative points, which will play a key role in our test procedure in Sec. III-B. We summary the quantizing procedure QUANTIZE(e, V, N) in Algorithm 1. The basic idea is to first find the range of the stair levels, i.e., $[n_{\min}, n_{\max}]$ and then find τ_e^i for any level i in this range by solving an equation $c_e(t_e) = iV$.

Time Complexity: (i) When $n_{\min} = n_{\max}$ (e.g., if $t_e^{\text{ub}} = t_e^{\text{lb}}$), the loop in lines 7-12 will not be executed. Thus, the total complexity of QUANTIZE(e, V, N) is $O(N)$ due to the initial loop in lines 1-3. (ii) When $n_{\min} < n_{\max}$, we need to solve an equation for each i in the range $[n_{\min}, n_{\max} - 1]$ as shown in line 8. Since we have assumed that $c_e(t_e)$ is a strictly decreasing function, we can use a binary search to solve this equation, which has time complexity $O\left(\log\left\lceil\frac{t_e^{\text{ub}} - t_e^{\text{lb}}}{\text{tol}}\right\rceil\right)$ where tol is the tolerance level for termination. The total complexity of QUANTIZE(e, V, N) is $O\left(N + (n_{\max} - n_{\min})\log\left\lceil\frac{t_e^{\text{ub}} - t_e^{\text{lb}}}{\text{tol}}\right\rceil\right) = O\left(N + N\log\left\lceil\frac{t_e^{\text{ub}} - t_e^{\text{lb}}}{\text{tol}}\right\rceil\right) = O\left(N\log\left(2\left\lceil\frac{t_e^{\text{ub}} - t_e^{\text{lb}}}{\text{tol}}\right\rceil\right)\right)$. To unify the expression of time complexity for both (i) and (ii), we define

$$\xi_e \triangleq \max\left\{2, 2\left\lceil\frac{t_e^{\text{ub}} - t_e^{\text{lb}}}{\text{tol}}\right\rceil\right\},$$

then the complexity of QUANTIZE(e, V, N) is $O(N \log \xi_e)$. Also, if we define

$$\xi \triangleq \max_{e \in \mathcal{E}} \xi_e, \quad (6)$$

then the complexity of QUANTIZE(e, V, N) is $O(N \log \xi)$ for any $e \in \mathcal{E}$.

Algorithm 1 A Quantizing Procedure $\text{QUANTIZE}(e, V, N)$

1: **for** $i = 1, 2, \cdots, N$ **do**
2:     Set $\tau_e^i = \text{nan}$
3: **end for**
4: Set $n_{\min} = \tilde{c}_e(t_e^{\text{ub}}) = \min\{\lfloor \frac{c_e(t_e^{\text{ub}})}{V} \rfloor + 1, N\}$
5: Set $n_{\max} = \tilde{c}_e(t_e^{\text{lb}}) = \min\{\lfloor \frac{c_e(t_e^{\text{lb}})}{V} \rfloor + 1, N\}$
6: Set $\tau_e^{n_{\max}} = t_e^{\text{lb}}$
7: **for** $i = n_{\min}, n_{\min} + 1, \cdots, n_{\max} - 1$ **do**
8:     Solve the equation $c_e(t_e) = iV$ over $t_e \in [t_e^{\text{lb}}, t_e^{\text{ub}}]$
9:     **if** the equation has a solution t_e **then**
10:         Set $\tau_e^i = t_e$
11:     **end if**
12: **end for**
13: **return** $\boldsymbol{\tau}_e = (\tau_e^1, \tau_e^2, \cdots, \tau_e^N)$

Algorithm 2 A Test Procedure $\text{TEST}(L, U, \delta)$

1: Set $V = \frac{L\delta}{n+1}$
2: Set $N = \lfloor \frac{U}{V} \rfloor + n + 1$
3: **for** $e \in \mathcal{E}$ **do**
4:     Get $\boldsymbol{\tau}_e = \text{QUANTIZE}(e, V, N + 1)$
5: **end for**
6: Set $g_s(c) = 0, \forall c = 0, 1, \cdots, N$
7: Set $g_v(0) = \infty, \forall v \neq s, v \in \mathcal{V}$
8: **for** $c = 1, 2, \cdots, N$ **do**
9:     **for** $v \in \mathcal{V}$ **do**
10:         Set $g_v(c)$ according to (7)
11:     **end for**
12:     **if** $g_d(c) \leq T$ **then**
13:         **return** the corresponding path p and travel time set $\boldsymbol{t}_p = \{t_e : e \in p\}$
14:     **end if**
15: **end for**
16: **return** FAIL

B. The Test Procedure

As introduced above, the test procedure should "approximately" compare S and the optimal value OPT such that it can answer either OPT $> S$ or OPT $\leq (1 + \delta)S$ in polynomial time. Inspired by [51], which improves the FPTAS of RSP in [24], we adopt a more powerful test procedure, denoted by $\text{TEST}(L, U, \delta)$. It can answer either OPT $> U$ or OPT $\leq U + \delta L$. Clearly, if we set $L = U = V$, $\text{TEST}(S, S, \delta)$ can answer either OPT $> S$ or OPT $\leq (1 + \delta)S$, which exactly completes the "approximate" comparison. The reason to adopt a more powerful test procedure, similar to [51], is that we will also use it to finally output a $(1 + \epsilon)$-approximate solution. We will discuss it soon in Sec. III-C.

The details of $\text{TEST}(L, U, \delta)$ are shown in Algorithm 2. As we mentioned before, the major difference between our problem PASO and the existing problem RSP is that PASO has a continuous fuel-time function for each edge instead of a fixed cost. Thus, different from the test procedure for RSP (see [51, Fig. 1]), we have a step to invoke the quantizing procedure (Algorithm 1) to quantize the fuel-time function, as shown in lines 3-5 in Algorithm 2. More importantly, since our test procedure $\text{TEST}(L, U, \delta)$ aims to check either OPT $> U$ or OPT $\leq U + \delta L$, roughly speaking, we do not need to quantize the portion of each fuel-time function with high fuel cost, i.e., larger than $U + \delta L$. Hence, to ensure polynomial time complexity eventually, we put a ceil $V(N + 1)$ for $c_e(t_e)$ as shown in line 4 of the algorithm, where V and N are appropriately set such that $V(N + 1) \geq U + \delta L$.

After such quantization, the fuel-time function $c_e(t_e)$ for each edge e consists of at most $N + 1$ representative points. Therefore, conceptually we can construct a new graph $\tilde{\mathcal{G}} = (\mathcal{V}, \tilde{\mathcal{E}})$. Each edge $e \in \mathcal{E}$ in the original graph corresponds to at most $N + 1$ edges in the new graph $\tilde{\mathcal{E}}$. For each edge $e \in \tilde{\mathcal{E}}$, the edge cost $\tilde{c}_e$ is a positive integer, as shown in (5). This is exactly an RSP problem. Therefore, the remaining steps follow the test procedure for RSP on the new graph $\tilde{\mathcal{G}}$. Specifically, since each edge $e \in \mathcal{E}$ has at most $N + 1$ possible cost values all of which are positive integers (each edge e in the new graph $\tilde{\mathcal{E}}$ has a positive integer cost), we can use dynamic programming to complete such test. Similar to [24], [51], we define $g_v(c)$ as the minimum path travel time

among all $s - v$ paths whose path cost is at most $c \in \mathbb{Z}^+$, and define $g_v(c) = \infty$ if no such path. The optimality condition (or Bellman's equation) becomes, for any $c = 1, 2, \cdots$,

$$g_v(c) = \min\{g_v(c - 1),$$
$$\min_{u, i: e = (u, v) \in \mathcal{E}, i = 1, \cdots, N, \tau_e^i \neq \text{nan}} \{g_u(c - i) + \tau_e^i\}\} \quad (7)$$

which is shown in line 10 in Algorithm 2. Since we only need to answer either OPT $> U$ or OPT $\leq U + \delta L$, we do not have to process large c. Instead, iterating c from 1 to N is enough for us to complete this task. This dynamic programming procedure is shown in lines 6-15 of Algorithm 2.

In PASO, we should carefully design the quantizing and the dynamic programming procedures jointly to guarantee performance, as shown in the following lemmas, which are the counterparts to Lemma 2 and Lemma 3 for RSP in [51].

Lemma 3: If Algorithm 2 returns a path p and travel time set $\boldsymbol{t}_p$, then we have

$$\text{OPT} \leq c(p, \boldsymbol{t}_p) \leq U + L\delta. \quad (8)$$

Proof: See Append. D in the supplementary materials. ∎

Lemma 4: If $U \geq \text{OPT}$, then Algorithm 2 must return a feasible path p and travel time set $\boldsymbol{t}_p$, which satisfy

$$c(p, \boldsymbol{t}_p) \leq \text{OPT} + L\delta. \quad (9)$$

Proof: See Append. E in the supplementary materials. ∎

Lemma 5: If Algorithm 2 returns FAIL, then we have

$$\text{OPT} > U. \quad (10)$$

Proof: This directly follows Lemma 4. ∎

Our test procedure either returns a path p and travel time set $\boldsymbol{t}_p$ in line 13, which implies that OPT $\leq U + L\delta$ from Lemma 3, or returns FAIL in line 16, which implies OPT $> U$ from Lemma 5. Therefore, Lemma 3 and Lemma 5 justify that our test procedure (Algorithm 2) completes the "approximate" comparison, i.e., answers either OPT $> U$ or OPT $\leq U + L\delta$.

Thus, for the purpose of the test procedure, Lemma 3 and Lemma 5 are enough. However, we present Lemma 4, which

---

Algorithm 3 An FPTAS

1: Get a lower bound LB and upper bound UB for OPT
2: Set $B_L = $ LB
3: Set $B_U = $ UB
4: **while** $\frac{B_U}{B_L} > 16$ **do**
5:     $S = \sqrt{B_L \cdot B_U}$
6:     Call TEST$(S, S, 1)$
7:     **if** TEST$(S, S, 1)$ returns FAIL **then**
8:        Set $B_L = S$
9:     **else**
10:       Set $B_U = 2S$
11:     **end if**
12: **end while**
13: Call TEST(B_L, B_U, ϵ)

---

is stronger than Lemma 5, to provide a sufficient condition such that our test procedure returns a path p and travel time set $\boldsymbol{t}_p$. We will use Lemma 4 shortly in Sec. III-C to finally output a $(1 + \epsilon)$-approximate solution.

Time Complexity: The quantizing procedures for all edges in lines 3-5 require $O(mN \log \xi)$. The dynamic programming procedure in lines 6-15 requires $O(mN^2)$. Since $N = \lfloor \frac{U}{V} \rfloor + n + 1 = \lfloor \frac{U}{L} \cdot \frac{n+1}{\delta} \rfloor + n + 1 = O(\frac{U}{L} \cdot \frac{n}{\delta} + n)$, the total time complexity of Algorithm 2 is $O(mN \log \xi + mN^2) = O(m(\frac{U}{L} \cdot \frac{n}{\delta} + n) \log \xi + m(\frac{U}{L} \cdot \frac{n}{\delta} + n)^2)$.

C. The Proposed FPTAS

Based on our own test procedure (Algorithm 2), we then follow the FPTAS for RSP in [51, Fig. 2] by replacing its test procedure with ours. For completeness, we present the FPTAS in Algorithm 3 and explain it with the following three steps.

Step 1 (line 1): To initialize the bound interval, we need to first obtain a lower bound LB and an upper bound UB for the optimal value OPT. Define that the minimum single-edge fuel cost is $\mathsf{C}^{\mathsf{lb}} \triangleq \min_{e \in \mathcal{E}} c_e(t_e^{\mathsf{ub}})$ and the maximum single-edge fuel cost is $\mathsf{C}^{\mathsf{ub}} \triangleq \max_{e \in \mathcal{E}} c_e(t_e^{\mathsf{lb}})$. Simply, we can use the minimum single-edge fuel consumption C^{lb} as the lower bound LB and use the maximum single-path[4] fuel consumption $n\mathsf{C}^{\mathsf{ub}}$ as the upper bound UB. Also, in Sec. IV, we will propose a heuristic scheme which can always output a set of LB and UB.

Step 2 (lines 2-12): Using the initial lower bound LB and upper bound UB, we design a binary search scheme, which repeatedly invokes our test procedure (Algorithm 2) to exponentially narrow down the bound interval $[B_L, B_U]$ until $B_U/B_L \leq 16$. The binary search step is visualized in Fig. 3. Note that we always keep B_L as a lower bound and B_U as an upper bound for OPT. Whenever $B_U/B_L > 16$, we input the geometric mean $S = \sqrt{B_L \cdot B_U}$ and $\delta = 1$ to the test procedure, as shown in lines 5 and 6. If TEST$(S, S, 1)$ returns FAIL, then according to Lemma 4, we must have $S < $ OPT. In this case, we reset the lower bound B_L to be S in line 8. Otherwise, TEST$(S, S, 1)$ returns a feasible path p and travel time set $\boldsymbol{t}_p$. According to Lemma 3, we must have

---

[4]A simple path can have at most n edges.

OPT $\leq S + \delta S = 2S$. We reset the upper bound to be $2S$ in line 10. It can be easily shown that this binary search returns a lower bound B_L and an upper bound B_U for OPT such that $B_U/B_L \leq 16$ in $O(\log \log \frac{\mathsf{UB}}{\mathsf{LB}})$ iterations.

Step 3 (line 13): When $\frac{B_U}{B_L} \leq 16$, we call our test procedure again but we use $L = B_L$ and $U = B_U$ and $\delta = \epsilon$. Since $B_U \geq $ OPT, according to Lemma 4, TEST(B_L, B_U, ϵ) must return a feasible path p and travel time $\boldsymbol{t}_p$ such that

$$c(p, \boldsymbol{t}_p) \leq \mathsf{OPT} + \epsilon B_L \leq \mathsf{OPT} + \epsilon\mathsf{OPT} = (1 + \epsilon)\mathsf{OPT}.$$

Therefore, we get a $(1 + \epsilon)$-approximate solution to PASO.

Time Complexity: *Step 1* requires $O(m)$ to get an initial lower bound LB and upper bound UB. *Step 2* invokes the test procedure $O(\log \log \frac{\mathsf{UB}}{\mathsf{LB}})$ times and each invoke takes $O(mn \log \xi + mn^2)$ time by using $L = U = S$ and $\delta = 1$. Thus *Step 2* takes $O((mn \log \xi + mn^2) \log \log \frac{\mathsf{UB}}{\mathsf{LB}})$. *Step 3* also invokes the test procedure, and it takes $O(\frac{mn \log \xi}{\epsilon} + \frac{mn^2}{\epsilon^2})$ time by using $\delta = \epsilon < 1$ and $O(\frac{U}{L}) = O(\frac{B_U}{B_L}) = O(1)$ because $\frac{B_U}{B_L} \leq 16 = O(1)$. Here we can also see why we need to use a binary search to obtain $\frac{B_U}{B_L} \leq 16$ in *Step 2*. This is because $\frac{B_U}{B_L} = O(1)$ ensures polynomial time complexity in *Step 3*. Therefore, the total complexity is $O((mn \log \xi + mn^2) \log \log \frac{\mathsf{UB}}{\mathsf{LB}} + \frac{mn \log \xi}{\epsilon} + \frac{mn^2}{\epsilon^2})$.

We summarize our results for the approximate scheme in the following theorem.

Theorem 2: Algorithm 3 returns a $(1 + \epsilon)$-approximate solution for PASO in time $O((mn \log \xi + mn^2) \log \log \frac{\mathsf{UB}}{\mathsf{LB}} + \frac{mn \log \xi}{\epsilon} + \frac{mn^2}{\epsilon^2})$. In addition, under our assumption that any edge-e fuel-rate-speed function $f_e(\cdot)$ is a polynomial function (see Sec. II-A), when we use LB $= \mathsf{C}^{\mathsf{lb}}$ and UB $= n\mathsf{C}^{\mathsf{ub}}$ where $\mathsf{C}^{\mathsf{lb}} \triangleq \min_{e \in \mathcal{E}} c_e(t_e^{\mathsf{ub}})$ and $\mathsf{C}^{\mathsf{ub}} \triangleq \max_{e \in \mathcal{E}} c_e(t_e^{\mathsf{lb}}) = c_{e_1}(t_{e_1}^{\mathsf{lb}})$, we have $\log \log \frac{\mathsf{UB}}{\mathsf{LB}} = \max\{O(\log \log n), O(I_{e_1})\}$ where I_{e_1} is the input size of all parameters of edge e_1. Thus, Algorithm 3 has time complexity polynomial in the input size of the problem PASO and $\frac{1}{\epsilon}$ and therefore is an FPTAS.

Proof: See Append. F in the supplementary materials. ∎

Although we generalize the FPTAS design from RSP to PASO, such an FPTAS (Algorithm 3) still has high complexity for a large-scale highway network with tens of thousands of nodes and edges. In the next section, we propose a heuristic scheme with substantially lower complexity.

IV. A FAST DUAL-BASED HEURISTIC

In this section, we present a heuristic scheme for our problem PASO based on Lagrangian relaxation. Such a heuristic scheme, as we will show later in Sec. IV-C, runs much faster than the FPTAS (Algorithm 3). Also, it always outputs a lower bound LB and an upper bound UB on OPT, which implements *Step 1* in Algorithm 3. Moreover, in most practical scenarios as shown in Sec. V, this heuristic scheme outputs an optimal (or at least near optimal) solution, i.e., LB $=$ UB $=$ OPT (or at least LB $\approx$ OPT $\approx$ UB).

A. Lagrangian Relaxation and Dual Problem

In our problem PASO, since the hard deadline constraint (4) couples path selection variable $\boldsymbol{x}$ with speed optimization

variable $\boldsymbol{t}$, we relax it and introduce a Lagrangian dual variable $\lambda \geq 0$, which can be interpreted as a (per-unit) delay price *over the entire network*.

Based on such relaxation, we can get the corresponding Lagrangian,

$$
\begin{aligned}
L(\boldsymbol{x}, \boldsymbol{t}, \lambda) &\triangleq \sum_{e \in \mathcal{E}} x_e \cdot c_e(t_e) + \lambda(\sum_{e \in \mathcal{E}} x_e t_e - T) \\
&= \sum_{e \in \mathcal{E}} x_e \cdot (c_e(t_e) + \lambda t_e) - \lambda T, \quad (11)
\end{aligned}
$$

and the corresponding dual function is defined as $D(\lambda) \triangleq \min_{\boldsymbol{x} \in \mathcal{X}, \boldsymbol{t} \in \mathcal{T}} L(\boldsymbol{x}, \boldsymbol{t}, \lambda)$. Then the dual problem of PASO is formulated as

$$
(\text{PASO-Dual}) \qquad \max_{\lambda \geq 0} D(\lambda)
$$

B. Obtain Dual Function

Before we solve the dual problem, let us first show how to obtain the dual function for a given λ as follows,

$$
\begin{aligned}
D(\lambda) &= \min_{\boldsymbol{x} \in \mathcal{X}, \boldsymbol{t} \in \mathcal{T}} L(\boldsymbol{x}, \boldsymbol{t}, \lambda) \\
&= -\lambda T + \min_{\boldsymbol{x} \in \mathcal{X}, \boldsymbol{t} \in \mathcal{T}} \sum_{e \in \mathcal{E}} x_e \cdot (c_e(t_e) + \lambda t_e) \\
&\stackrel{(E_1)}{=} -\lambda T + \min_{\boldsymbol{x} \in \mathcal{X}} \left[\min_{\boldsymbol{t} \in \mathcal{T}} \sum_{e \in \mathcal{E}} x_e \cdot (c_e(t_e) + \lambda t_e) \right] \\
&\stackrel{(E_2)}{=} -\lambda T + \min_{\boldsymbol{x} \in \mathcal{X}} \sum_{e \in \mathcal{E}} x_e \cdot \min_{t_e^{\text{lb}} \leq t_e \leq t_e^{\text{ub}}} (c_e(t_e) + \lambda t_e) \\
&\stackrel{(E_3)}{=} -\lambda T + \min_{\boldsymbol{x} \in \mathcal{X}} \sum_{e \in \mathcal{E}} x_e \cdot [c_e(t_e^*(\lambda)) + \lambda t_e^*(\lambda)] \\
&\stackrel{(E_4)}{=} -\lambda T + \min_{\boldsymbol{x} \in \mathcal{X}} \sum_{e \in \mathcal{E}} x_e \cdot w_e(\lambda) \\
&\stackrel{(E_5)}{=} -\lambda T + \sum_{e \in p^*(\lambda)} w_e(\lambda). \quad (12)
\end{aligned}
$$

We explain $(E_1) - (E_5)$ in (12) one by one. Equality (E_1) is because no coupled constraints exist for $\boldsymbol{x}$ and $\boldsymbol{t}$. Equality (E_2) is because no coupled constraints exist for the travel time at different edges in $\mathcal{T}$.

In equality (E_3), $t_e^*(\lambda)$ is defined as

$$
t_e^*(\lambda) \triangleq \arg \min_{t_e^{\text{lb}} \leq t_e \leq t_e^{\text{ub}}} (c_e(t_e) + \lambda t_e). \quad (13)
$$

Note that since we have assumed that $c_e(t_e)$ is strictly convex and strictly decreasing over $[t_e^{\text{lb}}, t_e^{\text{ub}}]$ in Sec. II-D, $t_e^*(\lambda)$ is unique and thus (13) is well defined. Specifically, $t_e^*(\lambda)$ can be obtained analytically as follows.

Lemma 6: Define $c_e'^{-1}(\cdot)$ as the inverse function of $c_e'(\cdot)$. Then we have

$$
t_e^*(\lambda) = \begin{cases} t_e^{\text{ub}}, & \text{If } 0 \leq \lambda < -c_e'(t_e^{\text{ub}}); \\ c_e'^{-1}(-\lambda), & \text{If } -c_e'(t_e^{\text{ub}}) \leq \lambda \leq -c_e'(t_e^{\text{lb}}); \quad (14) \\ t_e^{\text{lb}}, & \text{If } \lambda > -c_e'(t_e^{\text{lb}}). \end{cases}
$$

Proof: See Append. G in the supplementary materials. ∎

Now let us consider the complexity of computing $t_e^*(\lambda)$ based on Lemma 6. Since we assume that $f_e(\cdot)$ is a polynomial function in Sec. II-A and we define $c_e(t_e) = t_e \cdot f_e\left(\frac{D_e}{t_e}\right)$ in (2), then we can easily evaluate $c_e'(t_e)$ for any t_e. Thus, we can first determine the region that λ belongs to. Then,

- If $0 \leq \lambda < -c_e'(t_e^{\text{ub}})$, we obtain $t_e^*(\lambda) = t_e^{\text{ub}}$ with time complexity $O(1)$.
- If $\lambda > -c_e'(t_e^{\text{lb}})$, we obtain $t_e^*(\lambda) = t_e^{\text{lb}}$ with time complexity $O(1)$.
- If $-c_e'(t_e^{\text{ub}}) \leq \lambda \leq -c_e'(t_e^{\text{lb}})$, however, we cannot directly get $c_e'^{-1}(-\lambda)$ because the inverse function $c_e'^{-1}(\cdot)$ is not easy to evaluate. Instead of directly evaluating the inverse function, we find a t_e such that $c_e'(t_e) = -\lambda$ and such a t_e becomes $t_e^*(\lambda)$. Since $c_e'(\cdot)$ is a strictly increasing function due to the strict convexity of $c_e(\cdot)$, numerically we can design a binary search scheme to obtain $t_e^*(\lambda)$, whose time complexity is $O\left(\log \left\lceil \frac{t_e^{\text{ub}} - t_e^{\text{lb}}}{\text{tol}} \right\rceil \right) = O(\log \xi)$.

Overall, the time complexity to obtain $t_e^*(\lambda)$ is $O(\log \xi)$.

In addition, (13) has a nice economic interpretation. As we have relaxed the hard deadline constraint, we penalize each edge e with a delay cost, which is the product of the travel time t_e and the (per-unit) delay price λ. Then for a given delay price λ, each edge selects the optimal travel time to minimize its *generalized* cost, including both fuel cost $c_e(t_e)$ and delay cost λt_e. Thus, $t_e^*(\lambda)$ is the *best response* of edge e for a given delay price λ.

In equality (E_4), $w_e(\lambda)$ is defined as

$$
w_e(\lambda) \triangleq c_e(t_e^*(\lambda)) + \lambda t_e^*(\lambda), \quad (15)
$$

which can be interpreted as the minimum generalized cost (including both fuel cost and delay cost) of edge e for a given delay price λ. Obviously, $w_e(\lambda)$ is the generalized cost under the best response $t_e^*(\lambda)$.

In equality (E_5), since $\mathcal{X}$ restricts that an $s - d$ path is selected, $\min_{\boldsymbol{x} \in \mathcal{X}} \sum_{e \in \mathcal{E}} x_e \cdot w_e(\lambda)$ is exactly a shortest path problem where each edge e has a generalized cost $w_e(\lambda)$. We define $p^*(\lambda)$ as the resulting shortest-generalized-cost path.

In summary, (12) shows that for any dual variable λ, we only need to solve a shortest path problem to obtain the dual function value $D(\lambda)$, which is much easier than PASO.

C. The Heuristic Algorithm

Our heuristic scheme relies on one key observation. Define

$$
\delta(\lambda) \triangleq \sum_{e \in p^*(\lambda)} t_e^*(\lambda), \quad (16)
$$

which is the total travel time of the resulting shortest-generalized-cost path $p^*(\lambda)$ for a given λ. Our key observation is the following theorem (see an example in Fig. 6).

Theorem 3: $\delta(\lambda)$ is non-increasing over $\lambda \in [0, +\infty)$.

Proof: See Append. H in the supplementary materials. ∎

Theorem 3 shows that increasing λ will decrease the total travel time of the selected path based on the best responses of all edges. Intuitively, since λ can be interpreted as a delay price, increasing λ will force all edges to select a shorter travel time and further force the resulting shortest-generalized-cost path to have a shorter travel time.

Based on Theorem 3, we can use a simple dual variable λ to *coordinate* the total travel time. For example, when $\delta(\lambda) > T$,

Algorithm 4 A Heuristic Scheme

1: Set $\lambda_L = 0$
2: Set $\lambda_U = \lambda_{\max}$
3: **while** $\lambda_U - \lambda_L >$ tol **do**
4:     Set $\lambda_0 = \frac{\lambda_L + \lambda_U}{2}$
5:     Get $t_e^*(\lambda_0)$ from Lemma 6 for all $e \in \mathcal{E}$
6:     Get $w_e(\lambda_0) = c_e(t_e^*(\lambda_0)) + \lambda_0 t_e^*(\lambda_0)$ for all $e \in \mathcal{E}$
7:     Get the shortest path $p^*(\lambda_0)$ in terms of $w_e(\lambda_0)$
8:     **if** $\delta(p^*(\lambda_0)) = T$ **then**
9:         **return** $(p^*(\lambda_0), \{t_e^*(\lambda_0)\})$
10:     **else if** $\delta(p^*(\lambda_0)) > T$ **then**
11:         Set $\lambda_L = \lambda_0$
12:         Set $p^*(\lambda_L) = p^*(\lambda_0)$
13:         Set $t_e^*(\lambda_L) = t_e^*(\lambda_0), \forall e \in \mathcal{E}$
14:     **else**
15:         Set $\lambda_U = \lambda_0$
16:         Set $p^*(\lambda_U) = p^*(\lambda_0)$
17:         Set $t_e^*(\lambda_U) = t_e^*(\lambda_0), \forall e \in \mathcal{E}$
18:     **end if**
19: **end while**
20: **return** $(p^*(\lambda_L), \{t_e^*(\lambda_L)\})$ and $(p^*(\lambda_U), \{t_e^*(\lambda_U)\})$

---

we can increase λ such that $\delta(\lambda)$ can be decreased to finally satisfy the hard deadline requirement. On the other hand, when $\delta(\lambda) < T$, it means that the truck travels very fast and there still exists some room to increase the travel time and thus decrease the fuel consumption. Then we decrease λ such that $\delta(\lambda)$ can be increased to reach T. This is called a *coordination mechanism* [52, Ch. 5.1.6]. Therefore, we aim to find a λ_0 such that $\delta(\lambda_0) = T$. However, our problem PASO is not convex but has a combinatorial difficulty. Thus it is not guaranteed to find such a λ_0. We thus call our binary search for λ_0 (Algorithm 4) as a heuristic scheme.

In Algorithm 4, we first set an initial lower bound $\lambda_L = 0$ and an initial upper bound $\lambda_U = \lambda_{\max}$ for the targeted λ_0. In practice, since we are considering the fuel consumption and λ can be interpreted as a delay price, $\lambda_{\max}$ can be reasonably set to be an upper bound of the fuel consumption per hour. In our simulation in Sec. V, we set $\lambda_{\max} = 100$, which works for all settings. Then we do binary search in lines 3-19, where tol in line 3 is the tolerance level for termination which is close to zero. During the binary search, based on the non-increasing property of $\delta(\lambda)$ (Theorem 3), we keep updating the lower bound λ_L and its corresponding solution $(p^*(\lambda_L), \{t_e^*(\lambda_L) : e \in p^*(\lambda_L)\})$, as well as the upper bound λ_U and its corresponding solution $(p^*(\lambda_U), \{t_e^*(\lambda_U) : e \in p^*(\lambda_U)\})$.

This algorithm has two possible results:
▷ **Case 1:** If it returns in line 9, then we have found a λ_0 such that $\delta(\lambda_0) = T$. We prove that the returned solution is optimal for PASO in Theorem 4.
▷ **Case 2:** If it returns in line 20, then we have found a λ_0 such that $\delta(\lambda_L) > T$ and $\delta(\lambda_U) < T$. With a small enough tolerance level tol, $\lambda_L = \lambda_0 - \text{tol}/2 \to \lambda_0^-$. Likewise, $\lambda_U = \lambda_0 + \text{tol}/2 \to \lambda_0^+$. Roughly speaking, this means that $\delta(\lambda)$ is not continuous at $\lambda = \lambda_0$. Although this return does not guarantee optimality, we prove in Theorem 5 that

the returned solutions $(p^*(\lambda_L), \{t_e^*(\lambda_L) : e \in p^*(\lambda_L)\})$ and $(p^*(\lambda_U), \{t_e^*(\lambda_U) : e \in p^*(\lambda_U)\})$ give a lower bound LB and an upper bound UB for OPT, respectively.

Theorem 4: If Algorithm 4 returns in line 9, then the returned solution $(p^*(\lambda_0), \{t_e^*(\lambda_0) : e \in p^*(\lambda_0)\})$ is an optimal solution of PASO.

    Proof: See Append. I in the supplementary materials. ∎
As a by-product, Theorem 4 also shows that the strong duality for the combinatorial problem PASO holds in this case. Also, λ_0 is the optimal solution to the dual problem PASO-Dual.

Theorem 5: If Algorithm 4 returns in line 20, and define LB $\triangleq \sum_{e \in p^*(\lambda_L)} c_e(t_e^*(\lambda_L))$ and UB $\triangleq \sum_{e \in p^*(\lambda_U)} c_e(t_e^*(\lambda_U))$, then we have LB $\leq$ OPT $\leq$ UB.

    Proof: See Append. J in the supplementary materials. ∎
The LB and UB returned by Algorithm 4 in line 20 can be used for *Step 1* of Algorithm 3. For the case that Algorithm 4 returns in line 9, we use the returned optimal solution as both a lower bound and an upper bound with LB = UB = OPT. After such unification, Algorithm 4 always outputs a LB and UB for the optimal solution OPT.

Time Complexity: In line 7 in Algorithm 4, we use Dijkstra's shortest-path algorithm with a min-priority queue, which is the fastest known algorithm for the single-source single-destination shortest path problem with time complexity $O(m + n \log n)$ [53]. Thus, in the while loop, each iteration requires $O(m \log \xi + m + n \log n)$ time. And since the total number of iterations is $O(\log \frac{\lambda_{\max}}{\text{tol}})$, Algorithm 4 has complexity $O(m \log \xi + m + n \log n) \log \frac{\lambda_{\max}}{\text{tol}})$, much faster than the FPTAS (Algorithm 3). We summarize the complexity result in the following theorem.

Theorem 6: The time complexity of Algorithm 4 is $O((m \log \xi + m + n \log n) \log \frac{\lambda_{\max}}{\text{tol}})$.

Remark: A similar dual-based heuristical approach for RSP is proposed in [26]. However, as mentioned in Sec. III, different from RSP, our problem PASO has an extra design space of speed optimization. Therefore, theoretically our contribution in this section is to generalize the dual-based heuristical design from RSP [26] to PASO.

V. PERFORMANCE EVALUATION

In this section, we use real-world data to evaluate the performance of our algorithms. Our objectives are threefold: (i) collect realistic dataset and model the fuel-rate-speed function, (ii) evaluate and compare the performance of our FPTAS and heuristic, (iii) compare our algorithms with baseline algorithms, including both shortest path algorithm and fastest path algorithm adapted from common practice, and (iv) investigate the energy-deadline tradeoff of long-haul heavy-duty trucks by evaluating how much fuel can be saved by increasing the hard deadline.

A. Dataset

Transportation Network: We construct the U.S. National Highway Systems (NHS) from the dataset of Clinched Highway Mapping (CHM) Project [54]. The whole highway
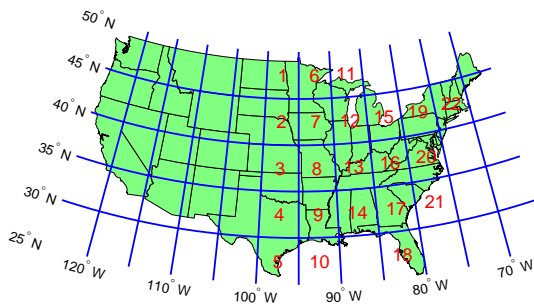
Fig. 4. U.S. map and 22 regions.

network graph file is specified in [55], which consists of 84504 nodes (waypoints) and 89119 (one-direction) edges.

Elevation: In this paper, we consider the grade/slope effect when modeling the road-dependent fuel-rate-speed function. To obtain the road grades, we use the Elevation Point Query Service [56] provided by the U.S. Geological Survey (USGS) to query elevations of all nodes in the NHS graph.

Speed Limits: We use the historical average speed as the maximum speed R_e^{ub} for each road e. HERE map [57] has put speed detectors over many countries including U.S., and it provides APIs to query location-based real-time speed information. We collect the real-time speed information from HERE map [57] for two weeks and use the average as R_e^{ub} for each road e in the NHS graph[5]. For the minimum speed limit R_e^{lb}, we manually set it to be $R_e^{\text{lb}} = \min\{30, R_e^{\text{ub}}\}$.

Fuel Consumption Data: It is hard for us to get suitable real-world fuel consumption data. In this paper, we instead leverage the widely-used ADVISOR simulator [58] to collect fuel consumption data (see Sec. V-B).

Heavy-Duty Truck: Fuel consumption highly depends on the truck type. Another benefit of using ADVISOR is that it also provides some heavy-duty truck configurations. In this simulation, we use the Kenworth T800 Vehicle [59], a Class 8 heavy-duty truck, with 36-ton full load. It is specified in files `VEH_KENT800Trailer.m` and `HeavyTruck_in.m`[6] in ADVISOR with the following parameters in Tab. III.

TABLE III
TRUCK PARAMETERS (KENWORTH T800).

| Drag Coefficient | Frontal area | Glider | Cargo |
c_d	A_f	Mass	Mass
0.7	8.5502 m^2	2,552kg	33,234kg

Preprocessing Highway Network: In the original NHS graph from CHM [55], we observe that: (i) most roads are in the "eastern" U.S., and (ii) many roads are very short with degree-1 endpoints (non-intersection roads). To create a network with more diverse paths, we first cut the whole NHS graph to the "eastern" part with longitude to the east of $100°W$ (see Fig. 4). We further merge the non-intersection roads with

---

[5]Due to the truck's gradeability, it may not achieve the average speed and thus later we also update R_e^{ub} based on the maximum speed that the truck can achieve at road e's grade.

[6]We replace `vinf.vehicle.name` by `VEH_KENT800Trailer`.

TABLE IV
NETWORK STATISTICS. "O" IS THE ORIGINAL NHS GRAPH, "E" IS THE "EASTERN" GRAPH (TO THE EAST OF $100°W$), AND "M" IS THE MERGED ONE. θ IS THE GRADE.

$\mathcal{G}$	n	m	avg D_e (mile)	avg R_e^{lb} (mph)	avg R_e^{ub} (mph)	avg $|\theta|$ (%)
O	84504	178238	2.08	37.4	55.97	0.64
E	65520	137521	1.97	37.3	55.55	0.58
M	38213	82781	3.26	36.43	54.19	0.82

the same level of grades[7] into a single road. Some network statistics after these two kinds of preprocessing are shown in Tab. IV. Note that since the average distance for each edge is 3.26 miles after preprocessing, it is reasonable to ignore the speed transition over two adjacent edges, which justifies the assumption in our fuel consumption model.

Moreover, to better visualize and evaluate the results, we divide the major "eastern" U.S. into 22 regions, as shown in Fig. 4. In each region $i \in [1, 22]$, we find the node in the graph which is nearest to the region's center. We also call it node i for convenience. Later on, we will use these 22 nodes as the source and destination nodes.

B. Model Fuel-Rate-Speed Function

We model the fuel-rate-speed function as

$$f_e(x) = a_e x^3 + b_e x^2 + c_e x + d_e, \forall e \in \mathcal{E} \tag{17}$$

Here x is the speed (unit: mph) and $f_e(x)$ is the fuel rate consumption (unit: gph (gallons per hour)). Although our model (17) can capture any road-dependent features/factors, e.g., grade, rolling resistance, and air density, etc., we only consider the road grade θ in this simulation, which is the major factor for truck fuel consumption [43].

To learn the parameters a_e, b_e, c_e and d_e in (17) in terms of functions of θ, we use ADVISOR by invoking function `adv_no_gui(action,input)` where we specify `action=drive_cycle` to run a driving cycle test [60, Ch. 2.3]. As mentioned in Sec. V-A, we choose the default vehicle file `HeavyTruck_in` where we use vehicle type `VEH_KENT800`, which specifies Kenworth T800 in Tab. III. For our purpose, we generate a driving cycle file where we use a constant speed (say x (mph)) profile over a total of 4 hours and a constant grade (say θ) over the whole speed profile. Then after running ADVISOR, we can get the total fuel consumption (say w (gallons)) over a 4-hour driving time with speed x over a grade-θ road. Since almost all the time the truck runs with constant speed x, we can get the corresponding fuel-rate consumption as $w/4$ (gph). By enumerating x from 10 mph to 70 mph with a step of 0.2 mph, and enumerating θ from -10.0% to 10.0% with a step of 0.1%, we collect many $(x, \theta, w/4)$ data points.

For each grade θ from -10.0% to 10.0% with a step of 0.1%, we use all $(x, w/4)$ points to fit the model (17) by invoking MATLAB's `fit` function. We sample several grade points in Tab. V, where we also put the strictly convex region for the fitted fuel-rate-speed function $f_e(x)$. As we can see, all

---

[7]In this simulation, we use 0.4% as the span of a grade level.

fuel-rate-speed functions $f_e(\cdot)$ are strictly convex in reasonable speed limit regions. For example, when grade is 0 (a flat road), $f_e(\cdot)$ is strictly convex if the speed is larger than 14.22 mph, which holds generally in reality. This justifies our assumption that the fuel-rate-speed function is polynomial and strictly convex over the speed limit region.

TABLE V

FITTING PARAMETERS. FOR THE CONVEX REGION, $\leq x$ IS THE INTERVAL $[0, x]$ AND $\geq x$ IS THE INTERVAL $[x, \infty)$.

Grade (%)	a_e	b_e	c_e	d_e	Convex Region
-2.0	5.5679e-06	-1.0839e-04	-0.0064	1.0655	≥ 6.49
-1.0	1.0778e-05	1.2960e-03	-0.0456	1.2879	≥ 0.00
0.0	3.3057e-05	-1.4102e-03	0.1476	0.5985	≥ 14.22
1.0	4.9559e-05	-2.3563e-03	0.2583	0.6624	≥ 15.85
2.0	5.9418e-05	-2.2194e-03	0.3404	0.8741	≥ 12.45

More concretely, we visualize the fuel-rate-speed function $f_e(x)$ and fuel-time function $c_e(t_e)$ for three sampled grades, -1.0%, 0.0%, and 1.0%, as shown in Fig. 5. We can see that both of them are strictly convex in reasonable regions. We also verify that $c_e(t_e)$ will first strictly decrease and then strictly increasing and thus we only need to focus on the decreasing interval without loss of optimality, as discussed in Sec. II-B. From Fig. 5(b), we also observe that the fuel-time curve is not smooth but has some glitches. This is due to the gear switch of the truck.
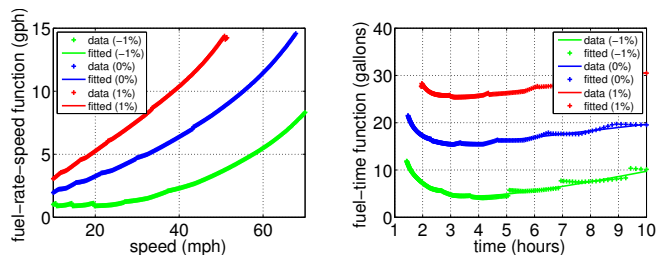

(a) Fuel-rate-speed function $f_e(x)$.　(b) Fuel-time function $c_e(t_e)$ over a 100-mile road.

Fig. 5. Fit curve v.s. data for grades 0%, $\pm 1\%$.

C. Evaluate/Compare FPTAS and Heuristic

We implement our algorithms with C++ where we use the SNAP graph structure [61]. We evaluate on a server with an 8-core Intel Core-i7 3770 3.4 Ghz CPU and 16 GB memory, running CentOS 6.4. To evaluate and compare our FPTAS (Algorithm 3) and heuristic scheme (Algorithm 4), we consider 4 different settings, S1, S2, S3, and S4, as shown in Tab. VI. Note that since we aim to compare them, we use LB $= 1$ and UB $= 1000$ in *Step 1* of Algorithm 3.

In terms of the minimized fuel cost of the algorithms, Tab. VI shows that the heuristic scheme always outputs the optimal solution (LB $=$ UB, hence LB $=$ UB $=$ OPT), and the FPTAS also outputs a near-optimal solution (e.g., in S1, 74.812 is only a little bit larger than OPT $= 74.811$). This demonstrates that both FPTAS and the heuristic scheme have good performance. However, in terms of time/space
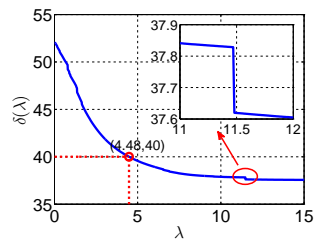
Fig. 6. An example for $\delta(\lambda)$ when $(s, d) = (4, 22)$.
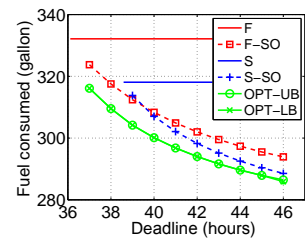
Fig. 7. The delay effect when $(s, d) = (9, 22)$.

complexity, the heuristic scheme is much better than FPTAS. As we can see, the FPTAS only works fine for the small-scale settings (S1 and S4), where the transportation network in regions 1 and 2 in Fig. 4 is considered, with only 1185 nodes and 2568 edges. When we use a little bit larger scale setting S2, it runs for nearly 1 hour and consumes 14.76 GB memory (out of 16 GB in total). Our server cannot run any other setting whose scale is larger than S2. We also note that the complexity of the FPTAS increases significantly as we decrease ϵ from 0.1 to 0.05, as shown in settings S1&S4. Contrarily, our heuristic scheme can handle all 22 regions (setting S3) with 38213 nodes and 82781 edges easily with low time/space complexity.

Tab. VI verifies that the FPTAS is not necessarily scalable to practical large-scale highway networks, but our heuristic scheme works very well in terms of both performance and complexity. To see why the heuristic scheme performs well, we examine an example source-destination pair in the setting S3, $(s, d) = (4, 22)$, and plot its $\delta(\lambda)$ function (the total travel time of the shortest-generalized-cost path, see (16)) in Fig. 6. We observe that function $\delta(\lambda)$ is non-increasing, which verifies Theorem 3. Moreover, $\delta(\lambda)$ has only a few small non-continuous jumps (e.g., a jump at point $\lambda = 11.47$ from 37.83 to 37.62). Whenever a (feasible) delay is not within such jump regions, we can always find a λ_0 such that $\delta(\lambda_0) = T$. According to Theorem 4, the output solution must be optimal. For example, when $T = 40$, we can find $\lambda_0 = 4.48$ such that $\delta(\lambda_0) = 40$, as shown in Fig. 6. The optimal solution can be derived as $(p^*(\lambda_0), \{t_e^*(\lambda_0)\})$. Even when T is within one of such jump regions (e.g., $T \in (37.62, 37.83)$), since the length of the deadline region (e.g., $(37.62, 37.83)$ has a length of 0.21 hours) is often negligible as compared to a nearly 40-hour travel, the output LB and UB would be very close. Hence, our heuristic scheme outputs an optimal (at least near-optimal) solution for any input T. We will further justify this observation with more instances in Sec. V-D.

D. Compare Performance with Baselines

In this section, we compare the performance of our heuristic scheme with four baseline algorithms. Let us first define *the fastest path* and *the shortest path*. *The fastest path* is the output path of any shortest path algorithm to the graph with edge-e cost $t_e^{\text{lb}}(= \frac{D_e}{R_e^{\text{ub}}})$ and *the shortest path* is the output path of any shortest path algorithm to the graph with edge-e cost D_e. Then the four baseline algorithms are as follows:

TABLE VI
COMPARISONS OF FPTAS AND HEURISTIC. HERE AN INSTANCE IS THE TUPLE (SOURCE, DESTINATION, DEADLINE), I.E., (s, d, T). FOR EXAMPLE, IN S1, (1,2,8) MEANS THAT THE SOURCE (RESP. DESTINATION) NODE IS 1 (RESP. 2), WHICH IS THE NEAREST NODE TO THE CENTER OF REGION 1 (RESP. REGION 2) IN FIG. 4, AND THE DEADLINE IS 8 HOURS.

No.	Network			Input		Performance (gallon)		Time (second)		Memory (GB)	
	Reg.	n	m	Instance	ϵ	Heuri. LB/UB	FPTAS	Heuri.	FPTAS	Heuri.	FPTAS
S1	1&2	1185	2568	(1,2,8)	0.1	74.811/74.811	74.812	1	50	0.29	2.73
S2	17&18	3274	7465	(18,17,10)	0.1	60.2795/60.2795	60.2798	2	3511	0.29	14.76
S3	1-22	38213	82781	(4,22,40)	0.1	290.744/290.744	-	365	-	0.29	-
S4	1&2	1185	2568	(1,2,8)	0.05	74.811/74.811	74.812	1	126	0.29	6.84

TABLE VII
DESCRIPTION OF 6 SOLUTIONS.

Solution	Description	Benchmark
F	Sol. of fastest path with maximum speed	Time
F-SO	Sol. of fastest path with optimal speed	-
S	Sol. of shortest path with maximum speed	Distance
S-SO	Sol. of shortest path with optimal speed	Distance
OPT-LB	Sol. of LB of our heuristic scheme	Fuel
OPT-UB	Sol. of UB of our heuristic scheme	-

TABLE VIII
PERFORMANCE OF INSTANCE $(s, d, T) = (9, 22, 40)$.

Sol.	Time (hour)	Incre. (%)	Dist. (mile)	Incre. (%)	Fuel (gal.)	Incre. (%)
F	36.11	-	1821	2.71	332.1	10.67
F-SO	40	10.76	1821	2.71	308.3	2.73
S	38.58	6.85	1773	-	318.0	5.99
S-SO	40	10.76	1773	-	307.0	2.30
OPT-LB	40	10.76	1778	0.30	300.1	-
OPT-UB	40	10.76	1778	0.30	300.1	0

(i) Fastest path algorithm with maximum speed: the path is the fastest path and the speed in each edge is the maximum speed.

(ii) Fastest path algorithm with optimal speed: the path is the fastest path and we further do speed optimization over the fastest path.

(iii) Shortest path algorithm with maximum speed: the path is the shortest path and the speed in each edge is the maximum speed.

(iv) Shortest path algorithm with optimal speed: the path is the shortest path and we further do speed optimization over the shortest path.

Each of them outputs one solution for PASO. Since our heuristic scheme outputs two solutions respectively corresponding to the LB and UB, we have 6 solutions in total, as summarized in Tab. VII.

In later comparison, since the travel time of F is the minimum time for any feasible solution of PASO, we will use it as the *time benchmark*. For example, a solution SOL (e.g., SOL could be OPT-UB) with time increment 10% means that $\frac{\text{Travel time of SOL} - \text{Travel time of F}}{\text{Travel time of F}} = 10\%$. Similarly, we use the travel distance of S/S-SO as the *distance benchmark*, and use the fuel consumption of OPT-LB as the *fuel benchmark*.

In our simulation, we evaluate in total 2704 different (s, d, T) tuples. The source node s and the destination node d could range from 1 to 22 (see the 22 regions in Fig. 4). For any (s, d) pair, the deadlines T could range from $\lceil T^{\text{f}} \rceil$ to $\lceil T^{\text{f}} \rceil + 9$ where T^{f} is the smallest travel time from s to d, i.e., the travel time computed by baseline algorithm (i).

A Single Instance: We first consider one instance $(s, d, T) = (9, 22, 40)$. Tab. VIII compares the 6 solutions. As we can see, our heuristic scheme again outputs the optimal solution. It consumes 300.1 gallons of fuel, runs 10.76% slower than the time benchmark (F), and 0.3% longer than the distance benchmark (S/S-SO). Also, without speed optimization, the fastest path (F) consumes 32 more gallons (10.67%) and the shortest path (S) consumers 18 more gallons (5.99%).

But with speed optimization, both fastest path and shortest path have near-optimal performance.

For $(s, d) = (9, 22)$, we also evaluate the effect of input deadline T as shown in Fig. 7. Considering speed optimization, when the input deadline $T \in [36.11, 38.58)$, the shortest path is infeasible, which shows that fastest path outperforms shortest path. The shortest path becomes feasible when $T \geq 38.58$, and it outperforms the fastest path when $T > 39$. This figure thus shows that the shortest path becomes better and better as the deadline constraint increases. Intuitively, when the hard deadline constraint can be satisfied, the travel distance would be critical for the total fuel consumption.

The OPT-UB curve in Fig. 7 is the *energy-deadline tradeoff* of $(s, d) = (9, 22)$. We see that increasing deadline can save fuel consumption, and the saving has a "diminishing return" property. For example, the truck can save 6.6 gallons of fuel if it increases its deadline from 37 to 38 hours, but the saving reduces to 1.46 gallons if its deadline is relaxed from 45 to 46 hours. A more comprehensive study on energy-deadline tradeoff is shown in Sec. V-E.

All Instances: Similar to Tab. VIII, we can get the time, distance, and fuel of the 6 solutions for all source-sink pairs. We evaluate the average performance of all running instances in terms of time/distance/fuel increments compared to the benchmark numbers, as summarized in Tab. IX. Note that in 4.84% of instances, shortest path is infeasible. Tab. IX only has the average performance over the instances where the shortest path is feasible.

Tab. IX shows that on average OPT-UB only consumes 0.02% of more fuels than the fuel benchmark (OPT-LB). This again shows that our heuristic scheme outputs a near-optimal solution in all instances.

For the baseline algorithms, Tab. IX shows that the fastest path (resp. shortest path) algorithm without speed optimization consumes 20.14% (resp. 16.40%) of more fuels than our solution. In other words, our heuristic solution achieves 16.76%

TABLE IX
AVERAGE PERFORMANCE OF ALL 2704 INSTANCES.

Sol.	Avg Time Incre.(%)	Avg Dist. Incre.(%)	Avg Fuel Incre.(%)	Avg Fuel Econ.(mpg)
F	-	1.71	20.14	5.05
F-SO	32.80	1.71	2.00	5.94
S	2.82	-	16.40	5.13
S-SO	32.80	-	0.31	5.94
OPT-LB	32.95	0.17	-	5.96
OPT-UB	32.89	0.18	0.02	5.96

(resp. 14.09%) fuel consumption reduction, as compared to the fastest path (resp. shortest path) algorithm. Our heuristic solution also improves the *36-ton*-truck's fuel economy from 5.05 for the fastest path and 5.13 for the shortest path to 5.96. Considering its significant portion of energy consumption, our solution can indeed save much fuel cost for the long-haul heavy-duty trucks.

When we allow speed optimization for the fastest path and the shortest path, we find that on average both of them are close to the optimal solution. More specifically, F-SO consumes 2.00% of more fuels and S-SO only consumes 0.31% of more fuels than OPT-LB. This apparently suggests that in the U.S., it is good enough to first choose the shortest or fastest path and then do speed optimization. However, in our simulation, the shortest path is infeasible among 4.84% of all instances, and the fastest path with speed optimization can consume 21.32% of more fuels in the worst instance. As opposed to them, our PASO solution is robust in the sense that it always output a solution that is both feasible and near-optimal. We also leave it as a future work to understand under which conditions the fastest/shortest path with speed optimization is close to the optimal solution.

E. Energy-Deadline Tradeoff

In this subsection, we evaluate all (s, d) pairs where s and d range from 1 to 22. For each (s, d) pair, we first get the smallest travel time T^f, i.e., the travel time computed by baseline algorithm (i) in Sec. V-D, and get the corresponding fuel consumption C^f. Now we increase the deadline by $x\%$ and evaluate the fuel consumption $C(x\%)$ when $T = (1+x\%)T^f$, and get the fuel consumption reduction $\frac{C^f - C(x\%)}{C^f}$. By changing the percentage of delay increase, i.e., x, we get different percentages of fuel consumption reduction. The energy-deadline tradeoff performance among all (s, d) pairs is shown in Fig. 8.

As we can see, the fuel consumption reduction has a "diminishing return" property. As compared to the fastest travel time, if we increase the hard deadline by 10%, we can reduce the fuel consumption by about 10% on average. If we increase the hard deadline by 50%, we can reduce the fuel consumption by about 20% on average. If we further increase the hard deadline after 70%, there is little extra benefit. This is because the optimal running speed over most edges becomes the minimum speed and there is little room to do further speed optimization if we increase the deadline more than 70%.
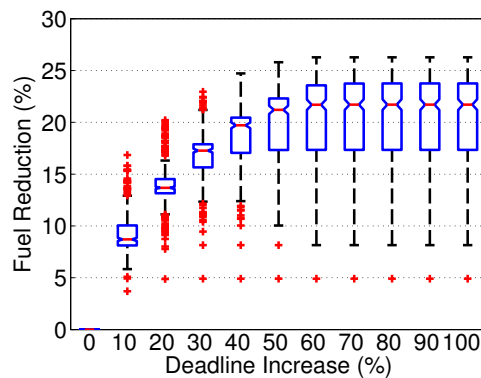

Fig. 8. The energy-deadline tradeoff.

VI. CONCLUSION AND FUTURE WORK

Provisioning both energy-efficient and timely delivery is of great importance for logistic operators. This paper presents a first step to study the energy-efficient timely transportation problem with an emphasis for long-haul heavy-duty trucks. We propose two algorithms: the first one is an FPTAS and the second one is a heuristic with lower complexity and near-optimal empirical performance. Our real-world data-driven simulations show that our solution guarantees timely delivery and can save up to 17% of fuel consumption as compared to a fastest/shortest path algorithm adapted from common practice. An interesting and important future direction is to generalize our results beyond the highway setting to cover more sophisticated local driving scenarios.

REFERENCES

[1] L. Deng, M. H. Hajiesmaili, M. Chen, and H. Zeng, "Energy-efficient timely transportation of long-haul heavy-duty trucks," in *Proc. ACM e-Energy*, 2016.

[2] Improving the fuel efficiency of American trucks, 2014. https://www.whitehouse.gov/the-press-office/2014/02/18/fact-sheet-opportunity-all-improving-fuel-efficiency-american-trucks-bol.

[3] S. C. Davis, S. W. Diegel, and R. G. Boundy, *Transportation Energy Data Book: Edition 34*. U.S. Department of Energy, 2015.

[4] Transportation overview. http://www.c2es.org/energy/use/transportation.

[5] W. Ford Torrey and D. Murray, "An analysis of the operational costs of trucking: A 2015 update," 2015.

[6] W. Harrington and A. Krupnick, "Improving fuel economy in heavy-duty vehicles," *Resources for the Future DP*, 2012.

[7] Z. Mohamed-Kassim and A. Filippone, "Fuel savings on a heavy vehicle via aerodynamic drag reduction," *Transportation Research Part D: Transport and Environment*, 2010.

[8] Supertruck team achieves 115% freight efficiency improvement in Class 8 long-haul truck, 2015. http://energy.gov/eere/vehicles/articles/supertruck-team-achieves-115-freight-efficiency-improvement-class-8-long-haul.

[9] Keeping your vehicle in shape. https://www.fueleconomy.gov/feg/maintain.jsp.

[10] F. Stodolsky, L. Gaines, and A. Vyas, "Analysis of technology options to reduce the fuel consumption of idling trucks," Argonne National Lab, Tech. Rep., 2000.

[11] A. A. Alam, A. Gattami, and K. H. Johansson, "An experimental study on the fuel reduction potential of heavy duty vehicle platooning," in *Prof. IEEE ITSC*, 2010.

[12] J. Larson, K.-Y. Liang, and K. H. Johansson, "A distributed framework for coordinated heavy-duty vehicle platooning," *IEEE Transactions on Intelligent Transportation Systems*, 2015.

[13] E. Demir, T. Bektaş, and G. Laporte, "A review of recent research on green road freight transportation," *European Journal of Operational Research*, 2014.

[14] Y. Suzuki, "A new truck-routing approach for reducing fuel consumption and pollutants emission," *Transportation Research Part D: Transport and Environment*, 2011.

[15] M. Tunnell, "Estimating truck-related fuel consumption and emissions in maine: A comparative analysis for six-axle, 100,000 pound vehicle configuration," in *Proc. TRB Annual Meeting*, 2011.

[16] E. Hellström, M. Ivarsson, J. Åslund, and L. Nielsen, "Look-ahead control for heavy trucks to minimize trip time and fuel consumption," *Control Engineering Practice*, 2009.

[17] E. Hellström, J. Åslund, and L. Nielsen, "Design of an efficient algorithm for fuel-optimal look-ahead control," *Control Engineering Practice*, 2010.

[18] Smarter trucking saves fuel over the long haul, 2011. http://news.nationalgeographic.com/news/energy/2011/09/110923-fuel-economy-for-trucks/.

[19] Fuel economy at various driving speeds. http://www.afdc.energy.gov/data/10312.

[20] W. Mallett, *Freight Performance Measurement: Travel Time in Freight-Significant Corridors*. U.S. Federal Highway Administration, 2006.

[21] Transportation logistics enhances your business efficiency, 2014. http://www.readytrucking.com/transportation-logistics-business-efficiency/.

[22] B. H. Ashby, *Protecting Perishable Foods during Transport by Truck*. U.S. Department of Agriculture, 2006.

[23] Place an order with guaranteed delivery. https://www.amazon.com/gp/help/customer/display.html?ref=hp_left_v4_sib?ie=UTF8&nodeId=201117390.

[24] R. Hassin, "Approximation schemes for the restricted shortest path problem," *Mathematics of Operations Research*, 1992.

[25] M. R. Garey and D. S. Johnson, *Computers and Intractability: A Guide to the Theory of NP-Completeness*, 1979.

[26] A. Jüttner, B. Szviatovski, I. Mécs, and Z. Rajkó, "Lagrange relaxation based method for the QoS routing problem," in *Proc. IEEE INFOCOM*, 2001.

[27] M. W. Savelsbergh, "Local search in routing problems with time windows," *Annals of Operations research*, vol. 4, no. 1, pp. 285–305, 1985.

[28] L. M. Gambardella, É. Taillard, and G. Agazzi, "Macs-vrptw: A multiple ant colony system for vehicle routing problems with time windows," 1999.

[29] J.-F. Cordeau, G. Laporte, and A. Mercier, "A unified tabu search heuristic for vehicle routing problems with time windows," *Journal of the Operational research society*, vol. 52, no. 8, pp. 928–936, 2001.

[30] K. C. Tan, L. H. Lee, Q. Zhu, and K. Ou, "Heuristic methods for vehicle routing problem with time windows," *Artificial intelligence in Engineering*, vol. 15, no. 3, pp. 281–295, 2001.

[31] J. Qian and R. Eglese, "Fuel emissions optimization in vehicle routing problems with time-varying speeds," *European Journal of Operational Research*, vol. 248, no. 3, pp. 840–848, 2016.

[32] I. Norstad, K. Fagerholt, and G. Laporte, "Tramp ship routing and scheduling with speed optimization," *Transportation Research Part C: Emerging Technologies*, vol. 19, no. 5, pp. 853–865, 2011.

[33] P. Serafini, "Some considerations about computational complexity for multi objective combinatorial problems," in *Recent advances and historical development of vector optimization*. Springer, 1987, pp. 222–232.

[34] G. Tsaggouris and C. Zaroliagis, "Multiobjective optimization: Improved fptas for shortest paths and non-linear objectives with applications," *Theory of Computing Systems*, vol. 45, no. 1, pp. 162–186, 2009.

[35] T. Breugem, T. Dollevoet, and W. van den Heuvel, "Analysis of fptases for the multi-objective shortest path problem," *Computers & Operations Research*, vol. 78, pp. 44–58, 2017.

[36] K. Ghoseiri and B. Nadjari, "An ant colony optimization algorithm for the bi-objective shortest path problem," *Applied Soft Computing*, vol. 10, no. 4, pp. 1237–1246, 2010.

[37] G. Scora, K. Boriboonsomsin, and M. Barth, "Value of eco-friendly route choice for heavy-duty trucks," *Research in Transportation Economics*, vol. 52, pp. 3–14, 2015.

[38] Energy consumption estimates by end-use sector, ranked by state, 2013. http://www.eia.gov/state/seds/data.cfm?incfile=/state/seds/sep_sum/html/rank_use.html&sid=US.

[39] N. T. Moungla, L. Létocart, and A. Nagih, "Solutions diversification in a column generation algorithm," *Algorithmic Operations Research*, vol. 5, no. 2, pp. 86–95, 2010.

[40] F. Vanderbeck, "Computational study of a column generation algorithm for bin packing and cutting stock problems," *Mathematical Programming*, vol. 86, no. 3, pp. 565–594, 1999.

[41] N. Ulder, E. Aarts, H.-J. Bandelt, P. van Laarhoven, and E. Pesch, "Genetic local search algorithms for the traveling salesman problem," *Parallel Problem Solving from Nature*, pp. 109–116, 1991.

[42] E. Demir, T. Bektaş, and G. Laporte, "A comparative analysis of several vehicle emission models for road freight transportation," *Transportation Research Part D: Transport and Environment*, 2011.

[43] K. Ahn, "Microscopic fuel consumption and emission modeling," Master's thesis, Virginia Polytechnic Institute and State University, 1998.

[44] D. J. Chang and E. K. Morlok, "Vehicle speed profiles to minimize work and fuel consumption," *Journal of Transportation Engineering*, vol. 131, no. 3, pp. 173–182, 2005.

[45] A. Fröberg, E. Hellström, and L. Nielsen, "Explicit fuel optimal speed profiles for heavy trucks on a set of topographic road profiles," SAE Technical Paper, Tech. Rep., 2006.

[46] G. Yang, H. Xu, Z. Wang, and Z. Tian, "Truck acceleration behavior study and acceleration lane length recommendations for metered on-ramps," *International Journal of Transportation Science and Technology*, vol. 5, no. 2, pp. 93–102, 2016.

[47] S. Ardekani, E. Hauer, and B. Jamei, "Traffic impact models," *Chapter 7 in Traffic Flow Theory, Oak Bridge National Laboratory Report*, 1992.

[48] F. An and M. Ross, "Model of fuel economy with applications to driving cycles and traffic management," *Transportation Research Record*, 1993.

[49] E. K. Nam and R. Giannelli, "Fuel consumption modeling of conventional and advanced technology vehicles in the physical emission rate estimator (PERE)," *U.S. Environmental Protection Agency*, 2005.

[50] I. M. Berry, "The effects of driving style and vehicle performance on the real-world fuel consumption of U.S. light-duty vehicles," Master's thesis, Massachusetts Institute of Technology, 2010.

[51] D. H. Lorenz and D. Raz, "A simple efficient approximation scheme for the restricted shortest path problem," *Operations Research Letters*, 2001.

[52] D. P. Bertsekas, *Nonlinear Programming*. Athena scientific, 1999.

[53] Dijkstra's algorithm. https://en.wikipedia.org/wiki/Dijkstra%27s_algorithm.

[54] J. D. Teresco. The Clinched Highway Mapping (CHM) project. http://cmap.m-plex.com/.

[55] CHM U.S. national highway systems. http://courses.teresco.org/chm/graphs/usa-national.gra.

[56] USGS elevation point query service. http://nationalmap.gov/epqs/.

[57] Traffic flow using corridor in HERE maps. https://developer.here.com/api-explorer/rest/traffic/flow-using-corridor.

[58] T. Markel, A. Brooker, T. Hendricks, V. Johnson, K. Kelly, B. Kramer, M. O'Keefe, S. Sprik, and K. Wipke, "ADVISOR: a systems analysis tool for advanced vehicle modeling," *Journal of Power Sources*, 2002.

[59] Kenworth T800 vehicle. http://www.kenworth.com/trucks/t800.

[60] ADVISOR documentation. http://adv-vehicle-sim.sourceforge.net/advisor_doc.html.

[61] J. Leskovec and R. Sosič. SNAP: A general purpose network analysis and graph mining library in C++, 2014. http://snap.stanford.edu/snap.

[62] F. Mannering, W. Kilareski, and S. Washburn, *Principles of Highway Engineering and Traffic Analysis*. John Wiley & Sons, 2007.

[63] A. Jeffrey and D. Zwillinger, *Table of Integrals, Series, and Products, Seventh Edition*. Academic Press, 2007.
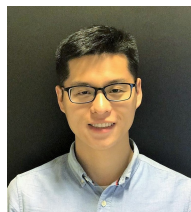
Lei Deng received his B.Eng. degree from the Department of Electronic Engineering, Shanghai Jiao Tong University, Shanghai, China in 2012 and his Ph.D. degree from the Department of Information Engineering, the Chinese University of Hong Kong, Hong Kong, China in 2017. From May 2015 to October 2015, he was a visiting scholar in School of Electrical and Computer Engineering, Purdue University, West Lafayette, IN, USA. His research interests are timely network communications, energy efficient timely transportation, and spectral-energy efficiency in wireless networks.

Mohammad H. Hajiesmaili received his B.Sc. degree in Computer Engineering from the Department of Computer Engineering, Sharif University of Technology, Iran, in 2007, and his M.Sc. and Ph.D. degrees in Computer Engineering from the Electrical and Computer Engineering Department, University of Tehran, Iran, in 2009 and 2014, respectively. He was a Postdoctoral Fellow with the Department of Information Engineering, the Chinese University of Hong Kong, from 2014 to 2016. He is currently a Postdoctoral Fellow with the Department of Electrical and Computer Engineering, Johns Hopkins University. His research interests include optimization, algorithm, and mechanism design in communication, energy, and transportation networks.

Minghua Chen (S'04 M'06 SM'13) received his B.Eng. and M.S. degrees from the Dept. of Electronic Engineering at Tsinghua University in 1999 and 2001, respectively. He received his Ph.D. degree from the Dept. of Electrical Engineering and Computer Sciences at University of California at Berkeley in 2006. He spent one year visiting Microsoft Research Redmond as a Postdoc Researcher. He joined the Dept. of Information Engineering, the Chinese University of Hong Kong in 2007, where he is currently an Associate Professor. He is also an Adjunct Associate Professor in Institute of Interdisciplinary Information Sciences, Tsinghua University. He received the Eli Jury award from UC Berkeley in 2007 (presented to a graduate student or recent alumnus for outstanding achievement in the area of Systems, Communications, Control, or Signal Processing) and The Chinese University of Hong Kong Young Researcher Award in 2013. He also received several best paper awards, including the IEEE ICME Best Paper Award in 2009, the IEEE Transactions on Multimedia Prize Paper Award in 2009, and the ACM Multimedia Best Paper Award in 2012. He is currently an Associate Editor of the IEEE/ACM Transactions on Networking. He serves as TPC Co-Chair of ACM e-Energy 2016 and General Chair of ACM e-Energy 2017. He receives the ACM Recognition of Service Award in 2017 for service contribution to the research community. His current research interests include energy systems (e.g., smart power grids and energy-efficient datacenters), intelligent transportation system, wireless networking, multimedia networking, online competitive optimization, distributed optimization, and delay-constrained network information flow.
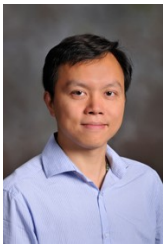
Haibo Zeng is currently an Assistant Professor at Virginia Tech, USA. He received his Ph.D. in Electrical Engineering and Computer Sciences from University of California at Berkeley. He was a senior researcher at General Motors R&D until October 2011, and an assistant professor at McGill University until August 2014. His research interests are design methodology, analysis, and optimization for embedded systems, cyber-physical systems, and real-time systems. He earned three best paper citations in the above fields.

Supplementary Materials

Appendix A
Physical Interpretation of Fuel-Rate-Speed Function

A truck running on a road with grade/slope θ (positive if moving up and negative if moving down) faces three resistances: aerodynamic (air) resistance, rolling resistance and grade resistance [62]. The air resistance is the friction of air, which is modeled as

$$F_a(v) = \frac{1}{2}\rho A_f c_d v^2, \tag{18}$$

where ρ is the air density and A_f the frontal area of the truck and c_d is drag coefficient of the truck (see Tab. III for c_d and A_f) and v is the speed of the truck. The rolling resistance is the friction between the tires and the ground, which is modeled as

$$F_r = c_r mg \cos\theta, \tag{19}$$

where c_r is the coefficient of rolling resistance (friction coefficient) between the tires and the ground, m is the truck mass and g is gravitational acceleration. The grade resistance is the force of the gravity on the opposite direction of truck movement, i.e.,

$$F_g = mg \sin\theta. \tag{20}$$

Then the tractive force is

$$F_t(v) = F_a(v) + F_r + F_g, \tag{21}$$

which yields to the power consumption

$$P_f(v) = F_t(v) \cdot v = \frac{1}{2}\rho A_f c_d v^3 + (c_r \cos\theta + \sin\theta)mgv. \tag{22}$$

We can regard $P_f(v)$ as the power demand to move the truck on the road with constant speed v. To provision such power demand, the internal combustion engine (ICE) needs to convert fuel into mechanical energy. There are a substantial number of models for ICE [49]. For the purpose of this physical interpretation, we use the following relationship (see [49, Equation 10]),

$$P_f = f(v) \cdot \mathsf{LHV} \cdot \eta, \tag{23}$$

where $f(v)$ is the fuel rate consumption (unit: gallon per hour), LHV is the lower heating value of the fuel (unit: KJ per gallon), and η is the fuel efficiency[8]. Eq. (23) gives the fuel-rate-speed function $f(v)$ as follows,

$$f(v) = \frac{P_f}{\mathsf{LHV} \cdot \eta} = \frac{\frac{1}{2}\rho A_f c_d v^3 + (c_r \cos\theta + \sin\theta)mgv}{\mathsf{LHV} \cdot \eta}, \tag{24}$$

which shows that the fuel-rate-speed function is polynomial with speed v and also strictly convex.

Therefore, such physical interpretation justifies our assumption for the fuel-rate-speed function in Sec. II-A.

---

[8]The unit of power demand P_f would be KW. We can appropriately make all units consistent.

Appendix B
Proof of Lemma 1

We can prove this lemma by using the continuous Jensen's inequality. For any speed profile $v : [0, t_e] \to \mathbb{R}^+$ over road/edge e, the incurred fuel consumption is $\int_0^{t_e} f_e(v(t))dt$, and the travelled distance is $\int_0^{t_e} v(t)dt$. As we require that the truck must pass edge e with exactly t_e hours, we must have

$$\int_0^{t_e} v(t)dt = D_e. \tag{25}$$

Since $f_e(\cdot)$ is convex, according to the continuous Jensen's inequality [63, Ch. 12.411], we have

$$\frac{\int_0^{t_e} f_e(v(t))dt}{t_e} \geq f_e\left(\frac{\int_0^{t_e} v(t)dt}{t_e}\right) = f_e\left(\frac{D_e}{t_e}\right), \tag{26}$$

which means

$$\int_0^{t_e} f_e(v(t))dt \geq t_e f_e\left(\frac{D_e}{t_e}\right), \tag{27}$$

with equality when $v(t) = \frac{D_e}{t_e}$ for all $t \in [0, t_e]$.

The proof is completed.

Appendix C
Proof of Lemma 2

Since the fuel-rate-speed function $f_e(v)$ is a polynomial function (and thus twice differentiable) with respect to v, we can thus obtain the first and second-order derivative of $c_e(t_e) = t_e f_e\left(\frac{D_e}{t_e}\right)$ with respect to t_e, i.e.,

$$c_e'(t_e) = f_e(\frac{D_e}{t_e}) - \frac{D_e}{t_e}f_e'(\frac{D_e}{t_e}), \tag{28}$$

and

$$\begin{aligned}c_e''(t_e) &= f_e'(\frac{D_e}{t_e})(-\frac{D_e}{t_e^2}) \\ &\quad -[(-\frac{D_e}{t_e^2})f_e'(\frac{D_e}{t_e}) + \frac{D_e}{t_e}f_e''(\frac{D_e}{t_e})(-\frac{D_e}{t_e^2})] \\ &= \frac{D_e^2}{t_e^3}f_e''(\frac{D_e}{t_e}).\end{aligned} \tag{29}$$

Since $f_e(\cdot)$ is strictly convex over the speed limit region, we have $f_e''(\frac{D_e}{t_e}) > 0$ and thus we conclude that

$$c_e''(t_e) > 0, \tag{30}$$

which proves that $c_e(\cdot)$ is strictly convex with respect to t_e over $[t_e^{\mathsf{lb}}, t_e^{\mathsf{ub}}]$.

For the second part of this lemma, we first observe that $c_e'(t_e)$ is a differentiable (and thus continuous) and strictly increasing function. Thus we will consider the following three cases.

Case 1 $0 \leq c_e'(t_e^{\mathsf{lb}})$: In this case, we know that $c_e(t_e)$ is strictly increasing over $[t_e^{\mathsf{lb}}, t_e^{\mathsf{ub}}]$ and we can set $\hat{t}_e = t_e^{\mathsf{lb}}$.

Case 2 $0 \in (c_e'(t_e^{\mathsf{lb}}), c_e'(t_e^{\mathsf{ub}}))$: In this case, we can find a $\hat{t}_e \in (c_e'(t_e^{\mathsf{lb}}), c_e'(t_e^{\mathsf{ub}}))$ such that $c_e'(\hat{t}_e) = 0$ due to the continuity of $c_e'(t_e)$.

Case 3 $0 \geq c_e'(t_e^{\mathsf{ub}})$: In this case, we know that $c_e(t_e)$ is strictly decreasing over $[t_e^{\mathsf{lb}}, t_e^{\mathsf{ub}}]$ and we can set $\hat{t}_e = t_e^{\mathsf{ub}}$.

In all three cases, we obtain that $c_e(t_e)$ is first strictly decreasing over $[t_e^{\text{lb}}, \hat{t}_e]$ and then strictly increasing over $[\hat{t}_e, t_e^{\text{ub}}]$. Note that $\hat{t}_e$ could be on the boundary of $[t_e^{\text{lb}}, t_e^{\text{ub}}]$, as shown in **Case 1** and **Case 3**.

The proof is completed.

APPENDIX D
PROOF OF LEMMA 3

First, since p and $\boldsymbol{t}_p$ is a feasible solution to PASO, we have $\text{OPT} \le c(p, \boldsymbol{t}_p)$.

Second, since Algorithm 2 returns in line 13, the path cost will be no greater than some $c \le N$, thus we have

$$\tilde{c}(p, \boldsymbol{t}_p) \triangleq \sum_{e \in p} \tilde{c}_e(t_e) = \sum_{e \in p} \min\{\lfloor \frac{c_e(t_e)}{V} \rfloor + 1, N+1\} \le N,$$

which clearly implies that

$$\tilde{c}_e(t_e) = \lfloor \frac{c_e(t_e)}{V} \rfloor + 1, \forall e \in p.$$

Then we have

$$
\begin{aligned}
\tilde{c}(p, \boldsymbol{t}_p) &= \sum_{e \in p} \tilde{c}_e(t_e) = \sum_{e \in p} \left[\lfloor \frac{c_e(t_e)}{V} \rfloor + 1 \right] \\
&\ge \sum_{e \in p} \frac{c_e(t_e)}{V} = \frac{c(p, t_p)}{V},
\end{aligned}
$$

which yields to

$$
\begin{aligned}
c(p, \boldsymbol{t}_p) &\le \tilde{c}(p, \boldsymbol{t}_p) V \le NV = \left(\lfloor \frac{U}{V} \rfloor + n + 1 \right) V \\
&\le \left(\frac{U}{V} + n + 1 \right) V = U + (n+1)V = U + L\delta.
\end{aligned}
$$

The proof is completed.

APPENDIX E
PROOF OF LEMMA 4

For PASO, let us denote $(p^*, \boldsymbol{t}_{p^*})$ as an optimal solution. Namely, p^* is an optimal path and $\boldsymbol{t}_{p^*}$ is the corresponding optimal travel time set. For each edge $e \in p^*$, we must have

$$\min\{\lfloor \frac{c_e(t_e)}{V} \rfloor + 1, N+1\} = \lfloor \frac{c_e(t_e)}{V} \rfloor + 1.$$

Suppose not. Then

$$\lfloor \frac{c_e(t_e)}{V} \rfloor + 1 > N + 1,$$

which means

$$c_e(t_e) \ge V \lfloor \frac{c_e(t_e)}{V} \rfloor > VN = V(\lfloor \frac{U}{V} \rfloor + n + 1) > U \ge \text{OPT}.$$

This is a contradiction to $c_e(t_e) \le \sum_{e \in p^*} c_e(t_e) = \text{OPT}$.

Then we have

$$
\begin{aligned}
\tilde{c}(p^*, \boldsymbol{t}_{p^*}) &= \sum_{e \in p^*} \tilde{c}_e(t_e) = \sum_{e \in p^*} \min\{\lfloor \frac{c_e(t_e)}{V} \rfloor + 1, N+1\} \\
&= \sum_{e \in p^*} \left[\lfloor \frac{c_e(t_e)}{V} \rfloor + 1 \right] \le \sum_{e \in p^*} \left[\frac{c_e(t_e)}{V} + 1 \right] \\
&\le \frac{\text{OPT}}{V} + n \le \frac{U}{V} + n \le (\lfloor \frac{U}{V} \rfloor + 1) + n = N.
\end{aligned}
\tag{31}
$$

Here is a critical step which is different from Lemma 3 in [51] for RSP problem. For each edge $e \in p^*$, t_e may not be a representative point in vector $\boldsymbol{\tau}_e$. However, we can consider the representative point $\tilde{t}_e = \tau_e^i$ where $i \triangleq \tilde{c}_e(t_e)$, which incurs the same fuel cost, i.e., $\tilde{c}_e(t_e) = \tilde{c}_e(\tilde{t}_e)$. Clearly, we also have $\tilde{c}(p^*, \tilde{\boldsymbol{t}}_{p^*}) \le N$ and $\tilde{t}_e \le t_e$ where $\tilde{\boldsymbol{t}}_{p^*} \triangleq \{\tilde{t}_e : e \in p^*\}$.

Therefore path p^* and travel time $\tilde{\boldsymbol{t}}_{p^*}$ must be examined by Algorithm 2, which completes the proof of the first part, i.e., Algorithm 2 must return a feasible path p and travel time $\boldsymbol{t}_p$. Moreover, we have

$$\tilde{c}(p, \boldsymbol{t}_p) \le \tilde{c}(p^*, \tilde{\boldsymbol{t}}_{p^*}) = \tilde{c}(p^*, \boldsymbol{t}_{p^*}). \tag{32}$$

From (31), we first note that

$$\tilde{c}(p^*, \boldsymbol{t}_{p^*}) \le \frac{\text{OPT}}{V} + n. \tag{33}$$

Second, since Algorithm 2 returns in line 13, we must have

$$\tilde{c}(p, \boldsymbol{t}_p) \triangleq \sum_{e \in p} \tilde{c}_e(t_e) = \sum_{e \in p} \min\{\lfloor \frac{c_e(t_e)}{V} \rfloor + 1, N+1\} \le N,$$

which clearly implies that

$$\tilde{c}_e(t_e) = \lfloor \frac{c_e(t_e)}{V} \rfloor + 1, \forall e \in p.$$

We then note that

$$
\begin{aligned}
\tilde{c}(p, \boldsymbol{t}_p) &= \sum_{e \in p} c_e(t_e) = \sum_{e \in p} \min\{\lfloor \frac{c_e(t_e)}{V} \rfloor + 1, N+1\} \\
&= \sum_{e \in p} \left(\lfloor \frac{c_e(t_e)}{V} \rfloor + 1 \right) \\
&\ge \sum_{e \in p} \left(\frac{c_e(t_e)}{V} \right) \\
&= \frac{c(p, \boldsymbol{t}_p)}{V}.
\end{aligned}
\tag{34}
$$

Inserting inequalities (33) and (34) into (32), we obtain

$$\frac{c(p, \boldsymbol{t}_p)}{V} \le \frac{\text{OPT}}{V} + n,$$

which means

$$c(p, \boldsymbol{t}_p) \le \text{OPT} + nV \le \text{OPT} + L\delta.$$

The proof is competed.

APPENDIX F
PROOF OF THEOREM 2

The first part of this theorem directly follow the analysis of *Steps 1-3* in Sec. III-C. Namely, Algorithm 3 returns a $(1+\epsilon)$-approximate solution for PASO in time

$$O((mn \log \xi + mn^2) \log \log \frac{\text{UB}}{\text{LB}} + \frac{mn \log \xi}{\epsilon} + \frac{mn^2}{\epsilon^2}). \tag{35}$$

Now we prove the second part of this theorem. Namely, if we use $\text{LB} = \text{C}^{\text{lb}}$ and $\text{UB} = n\text{C}^{\text{ub}}$ where $\text{C}^{\text{lb}} \triangleq \min_{e \in \mathcal{E}} c_e(t_e^{\text{ub}})$ and $\text{C}^{\text{ub}} \triangleq \max_{e \in \mathcal{E}} c_e(t_e^{\text{lb}})$, Algorithm 3 has time complexity polynomial in the input size of the problem PASO and therefore is an FPTAS. According to (35), we only need to show $\log \log \frac{\text{UB}}{\text{LB}} = \log \log \frac{n\text{C}^{\text{ub}}}{\text{C}^{\text{lb}}}$ is polynomial in the input size.

Suppose that $\mathsf{C}^{\mathsf{ub}} \triangleq \max_{e \in \mathcal{E}} c_e(t_e^{\mathsf{lb}}) = c_{e_1}(t_{e_1}^{\mathsf{lb}})$. For edge e_1, we should input all its properties, i.e., $\{D_{e_1}, R_{e_1}^{\mathsf{lb}}, R_{e_1}^{\mathsf{ub}}, f_{e_1}\}$ where f_{e_1} is a polynomial function. Suppose that

$$f_{e_1}(x) = a_1 x^{k_1} + a_2 x^{k_2} + \cdots + a_q x^{k_q}.$$

Then to input fuel-rate-speed function f_{e_1}, we only need to input $a_1, k_1, a_2, k_2, \cdots, a_q, k_q$. Therefore, for edge e_1, we should input the following real numbers,

$$\{D_{e_1}, R_{e_1}^{\mathsf{lb}}, R_{e_1}^{\mathsf{ub}}, a_1, k_1, a_2, k_2, \cdots, a_q, k_q\}.$$

The input size for edge e_1 is

$$I_{e_1} \geq \log \left(\frac{D_{e_1} + R_{e_1}^{\mathsf{lb}} + R_{e_1}^{\mathsf{ub}} + a_1 + k_1 + a_2 + k_2 + \cdots + a_q + k_q}{\mathsf{eps}} \right),$$

where $\mathsf{eps} \ll 1$ is the machine epsilon, i.e., the maximum relative error of for rounding a real number to the nearest floating point number that can be represented by a digital machine. Now let us show that $\log \log \frac{\mathsf{C}^{\mathsf{ub}}}{\mathsf{eps}}$ is polynomial in I_{e_1}.

According to the definition of the fuel-time function $c_{e_1}(\cdot)$ in (2), we get

$$\log \log \left(\frac{\mathsf{C}^{\mathsf{ub}}}{\mathsf{eps}} \right) = \log \log \left(\frac{c_{e_1}(t_{e_1}^{\mathsf{lb}})}{\mathsf{eps}} \right)$$

$$= \log \log \left(\frac{t_{e_1}^{\mathsf{lb}} \cdot f_{e_1}(\frac{D_{e_1}}{t_{e_1}^{\mathsf{lb}}})}{\mathsf{eps}} \right) = \log \log \left(\frac{\frac{D_{e_1}}{R_{e_1}^{\mathsf{ub}}} \cdot f_{e_1}(R_{e_1}^{\mathsf{ub}})}{\mathsf{eps}} \right)$$

$$= \log \left[\log \left(\frac{D_{e_1}}{R_{e_1}^{\mathsf{ub}}} \right) + \log \left(\frac{f_{e_1}(R_{e_1}^{\mathsf{ub}})}{\mathsf{eps}} \right) \right]$$

$$= \log \left[\log \left(\frac{D_{e_1}}{\mathsf{eps}} \right) - \log \left(\frac{R_{e_1}^{\mathsf{ub}}}{\mathsf{eps}} \right) + \log \left(\frac{f_{e_1}(R_{e_1}^{\mathsf{ub}})}{\mathsf{eps}} \right) \right]$$

$$\leq \log \left[I_{e_1} + \log \left(\frac{f_{e_1}(R_{e_1}^{\mathsf{ub}})}{\mathsf{eps}} \right) \right]$$

$$\text{(Since } R_{e_1}^{\mathsf{ub}} > 0 \text{ and thus } R_{e_1}^{\mathsf{ub}} \geq \mathsf{eps})$$

$$= \log \left[I_{e_1} + \log \left(\frac{a_1 (R_{e_1}^{\mathsf{ub}})^{k_1} + \cdots + a_q (R_{e_1}^{\mathsf{ub}})^{k_q}}{\mathsf{eps}} \right) \right]$$

$$\leq \log \left[I_{e_1} + \log \left(\frac{q a_i (R_{e_1}^{\mathsf{ub}})^{k_i}}{\mathsf{eps}} \right) \right]$$

$$\left(\text{Define } i \in \arg \max_{j \in [1,q]} a_j (R_{e_1}^{\mathsf{ub}})^{k_j} \right)$$

$$= \log \left[I_{e_1} + \log q + \log \left(\frac{a_i}{\mathsf{eps}} \right) + \log \left(\frac{(R_{e_1}^{\mathsf{ub}})^{k_i}}{\mathsf{eps}^{k_i}} \cdot \mathsf{eps}^{k_i} \right) \right]$$

$$\leq \log \left[I_{e_1} + I_{e_1} + I_{e_1} + k_i \log \left(\frac{R_{e_1}^{\mathsf{ub}}}{\mathsf{eps}} \right) \right]$$

$$\text{(Since } \log \mathsf{eps} < 0)$$

$$\leq \log \left[I_{e_1} + I_{e_1} + I_{e_1} + \frac{k_i}{\mathsf{eps}} \log \left(\frac{R_{e_1}^{\mathsf{ub}}}{\mathsf{eps}} \right) \right]$$

$$\text{(Since } \mathsf{eps} < 1)$$

$$\leq \log \left[I_{e_1} + I_{e_1} + I_{e_1} + \frac{k_i}{\mathsf{eps}} \cdot I_{e_1} \right]$$

$$\leq \log \left[I_{e_1} + I_{e_1} + I_{e_1} + 2^{I_{e_1}} \cdot I_{e_1} \right]$$

$$= \log I_{e_1} + \log(3 + 2^{I_{e_1}})$$

$$\leq \log I_{e_1} + \log(3 \cdot 2^{I_{e_1}} + 2^{I_{e_1}})$$

$$= \log I_{e_1} + I_{e_1} + 2 = O(I_{e_1}),$$

which is thus polynomial in I_{e_1}.

Then

$$\log \log \frac{n \mathsf{C}^{\mathsf{ub}}}{\mathsf{C}^{\mathsf{lb}}} = \log \log \frac{\frac{n \mathsf{C}^{\mathsf{ub}}}{\mathsf{eps}}}{\frac{\mathsf{C}^{\mathsf{lb}}}{\mathsf{eps}}} \leq \log \log \frac{n \mathsf{C}^{\mathsf{ub}}}{\mathsf{eps}}$$

$$= \log \left(\log n + \log \frac{\mathsf{C}^{\mathsf{ub}}}{\mathsf{eps}} \right)$$

$$\leq 2 \max \left\{ \log \log n, \log \log \frac{\mathsf{C}^{\mathsf{ub}}}{\mathsf{eps}} \right\}$$

$$= \max \{ O(\log \log n), O(I_{e_1}) \}, \tag{36}$$

which is polynomial in the input size of PASO because both $O(\log \log n)$ and $O(I_{e_1})$ are polynomial in the input size of PASO. We thus prove the second part of this theorem.

The proof is completed.

APPENDIX G
PROOF OF LEMMA 6

Define function $h(t_e) = c_e(t_e) + \lambda t_e$. Then we can get the first derivative as

$$h'(t_e) = c_e'(t_e) + \lambda. \tag{37}$$

Since $c_e(t_e)$ is a strictly convex and strict decreasing function, we know that $c_e'(t_e)$ (and also $h'(t_e)$) is a strictly increasing function and $c_e'(t_e) < 0$ at interval $[t_e^{\mathsf{lb}}, t_e^{\mathsf{ub}}]$. We then consider the following three cases.

Case 1: If $0 \leq \lambda < -c_e'(t_e^{\mathsf{ub}})$, we get that $c_e'(t_e^{\mathsf{ub}}) + \lambda < 0$ and thus

$$h'(t_e) \leq h'(t_e^{\mathsf{ub}}) < 0, \forall, t \in [t_e^{\mathsf{lb}}, t_e^{\mathsf{ub}}]. \tag{38}$$

This shows that $h(t_e)$ is strictly decreasing at $[t_e^{\mathsf{lb}}, t_e^{\mathsf{ub}}]$ and the minimal value is attained at $t_e^*(\lambda) = t_e^{\mathsf{ub}}$.

Case 2: If $-c_e'(t_e^{\mathsf{ub}}) \leq \lambda \leq -c_e'(t_e^{\mathsf{lb}})$, then we can get that $c_e'^{-1}(-\lambda) \in [t_e^{\mathsf{lb}}, t_e^{\mathsf{ub}}]$. Clearly, the monotonic increasing property of $h'(t_e)$ implies that $h'(t_e) < 0$ at $[t_e^{\mathsf{lb}}, c_e'^{-1}(-\lambda))$ and $h'(t_e) > 0$ at $(c_e'^{-1}(-\lambda), t_e^{\mathsf{lb}}]$. This means that the minimal value is attained at $t_e^*(\lambda) = c_e'^{-1}(-\lambda)$.

Case 3: If $\lambda > -c_e'(t_e^{\mathsf{lb}})$, we get that $c_e'(t_e^{\mathsf{lb}}) + \lambda > 0$ and thus

$$h'(t_e) \geq h'(t_e^{\mathsf{lb}}) > 0, \forall, t \in [t_e^{\mathsf{lb}}, t_e^{\mathsf{ub}}]. \tag{39}$$

This shows that $h(t_e)$ is strictly increasing at $[t_e^{\mathsf{lb}}, t_e^{\mathsf{ub}}]$ and the minimal value is attained at $t_e^*(\lambda) = t_e^{\mathsf{lb}}$.

The proof is completed.

APPENDIX H
PROOF OF THEOREM 3

Let us consider any two λ_1, λ_2 with $0 \leq \lambda_1 < \lambda_2$. We need to prove $\delta(\lambda_1) \geq \delta(\lambda_2)$. Suppose that the optimal path at λ_1 is $p^*(\lambda_1) = p_1$ and the optimal path at λ_2 is $p^*(\lambda_2) = p_2$[9].

For any path p and any $\lambda \geq 0$, we denote its (optimal) generalized path cost as

$$W_p(\lambda) \triangleq \sum_{e \in p} w_e(\lambda) = \sum_{e \in p} \left[c_e(t_e^*(\lambda)) + \lambda t_e^*(\lambda) \right], \quad (40)$$

and denote its corresponding path fuel cost as

$$C_p(\lambda) \triangleq \sum_{e \in p} c_e(t_e^*(\lambda)). \quad (41)$$

and denote its corresponding path delay

$$T_p(\lambda) \triangleq \sum_{e \in p} t_e^*(\lambda). \quad (42)$$

Clearly, we have $W_p(\lambda) = C_p(\lambda) + \lambda T_p(\lambda)$.

Based on such notations, we have $\delta(\lambda_1) = T_{p_1}(\lambda_1)$ and $\delta(\lambda_2) = T_{p_2}(\lambda_2)$, and we need to prove $T_{p_1}(\lambda_1) \geq T_{p_2}(\lambda_2)$.

When $\lambda = \lambda_1$, the optimal path is p_1, which means that

$$\begin{aligned} W_{p_1}(\lambda_1) &= C_{p_1}(\lambda_1) + \lambda_1 T_{p_1}(\lambda_1) \\ &\leq W_{p_2}(\lambda_1) = C_{p_2}(\lambda_1) + \lambda_1 T_{p_2}(\lambda_1) \end{aligned} \quad (43)$$

Similarly, when $\lambda = \lambda_2$, the optimal path is p_2, which means that

$$\begin{aligned} W_{p_2}(\lambda_2) &= C_{p_2}(\lambda_2) + \lambda_2 T_{p_2}(\lambda_2) \\ &\leq W_{p_1}(\lambda_2) = C_{p_1}(\lambda_2) + \lambda_2 T_{p_1}(\lambda_2) \end{aligned} \quad (44)$$

Now we will use the fact that $t_e^*(\lambda)$ minimizes $w_e(\lambda)$, as defined in (13). Since both $t_e^*(\lambda_1)$ and $t_e^*(\lambda_2)$ are feasible, i.e., in the interval $[t_e^{\text{lb}}, t_e^{\text{ub}}]$, we get that

$$\begin{aligned} W_{p_2}(\lambda_1) &= C_{p_2}(\lambda_1) + \lambda_1 T_{p_2}(\lambda_1) \\ &= \sum_{e \in p_2} (c_e(t_e^*(\lambda_1)) + \lambda_1 t_e^*(\lambda_1)) \\ &= \sum_{e \in p_2} \min_{t_e^{\text{lb}} \leq t_e \leq t_e^{\text{ub}}} (c_e(t_e) + \lambda_1 t_e) \\ &\leq \sum_{e \in p_2} (c_e(t_e^*(\lambda_2)) + \lambda_1 t_e^*(\lambda_2)) \\ &= C_{p_2}(\lambda_2) + \lambda_1 T_{p_2}(\lambda_2). \end{aligned} \quad (45)$$

Similarly, we have

$$W_{p_1}(\lambda_2) = C_{p_1}(\lambda_2) + \lambda_2 T_{p_1}(\lambda_2) \leq C_{p_1}(\lambda_1) + \lambda_2 T_{p_1}(\lambda_1). \quad (46)$$

Inserting (45) into (43), we get that

$$C_{p_1}(\lambda_1) + \lambda_1 T_{p_1}(\lambda_1) \leq C_{p_2}(\lambda_2) + \lambda_1 T_{p_2}(\lambda_2),$$

which implies that

$$\lambda_1 \left[T_{p_1}(\lambda_1) - T_{p_2}(\lambda_2) \right] \leq C_{p_2}(\lambda_2) - C_{p_1}(\lambda_1). \quad (47)$$

Similarly, inserting (46) into (44), we get that

$$C_{p_2}(\lambda_2) + \lambda_2 T_{p_2}(\lambda_2) \leq C_{p_1}(\lambda_1) + \lambda_2 T_{p_1}(\lambda_1),$$

[9]Paths p_1 and p_2 could be the same.

which implies that

$$-\lambda_2 \left[T_{p_1}(\lambda_1) - T_{p_2}(\lambda_2) \right] \leq C_{p_1}(\lambda_1) - C_{p_2}(\lambda_2). \quad (48)$$

Summing (47) and (48), we get that

$$(\lambda_1 - \lambda_2) \left[T_{p_1}(\lambda_1) - T_{p_2}(\lambda_2) \right] \leq 0. \quad (49)$$

Since we assume that $\lambda_1 < \lambda_2$, we must have

$$T_{p_1}(\lambda_1) \geq T_{p_2}(\lambda_2). \quad (50)$$

The proof is completed.

APPENDIX I
PROOF OF THEOREM 4

At the point λ_0, the dual function has value

$$\begin{aligned} D(\lambda_0) &= -\lambda_0 T + \min_{x \in \mathcal{X}} \sum_{e \in \mathcal{E}} x_e \cdot \min_{t_e^{\text{lb}} \leq t_e \leq t_e^{\text{ub}}} (c_e(t_e) + \lambda_0 t_e) \\ &= -\lambda_0 T + \min_{x \in \mathcal{X}} \sum_{e \in \mathcal{E}} x_e \cdot (c_e(t_e^*(\lambda_0)) + \lambda_0 t_e^*(\lambda_0)) \\ &= -\lambda_0 T + \sum_{e \in p^*(\lambda_0)} [c_e(t_e^*(\lambda_0)) + \lambda_0 t_e^*(\lambda_0)] \\ &= -\lambda_0 T + \sum_{e \in p^*(\lambda_0)} c_e(t_e^*(\lambda_0)) + \lambda_0 \sum_{e \in p^*(\lambda_0)} t_e^*(\lambda_0) \\ &= -\lambda_0 T + \lambda_0 \delta(\lambda_0) + \sum_{e \in p^*(\lambda_0)} c_e(t_e^*(\lambda_0)) \\ &= -\lambda_0 T + \lambda_0 T + \sum_{e \in p^*(\lambda_0)} c_e(t_e^*(\lambda_0)) \\ &= \sum_{e \in p^*(\lambda_0)} c_e(t_e^*(\lambda_0)). \end{aligned} \quad (51)$$

On one hand, we know that any dual function value will be a lower bound of OPT according to the weak duality. Thus,

$$D(\lambda_0) \leq \text{OPT}. \quad (52)$$

On the other hand, we know that $p^*(\lambda_0)$ is a feasible path and $\{t_e^*(\lambda_0), e \in p^*(\lambda_0)\}$ satisfies

$$\sum_{e \in p^*(\lambda_0)} t_e^*(\lambda_0) = T. \quad (53)$$

Here $p^*(\lambda_0)$ and $\{t_e^*(\lambda_0), e \in p^*(\lambda_0)\}$ is a feasible solution to PASO with the objective value $\sum_{e \in p^*(\lambda_0)} c_e(t_e^*(\lambda_0)) = D(\lambda_0)$, which is an upper bound of OPT, i.e.,

$$D(\lambda_0) \geq \text{OPT}. \quad (54)$$

Eq. (52) and (54) conclude that $D(\lambda_0) = \text{OPT}$, and $p^*(\lambda_0)$ and $\{t_e^*(\lambda_0), e \in p^*(\lambda_0)\}$ is an optimal solution to PASO.

The proof is completed.

APPENDIX J
PROOF OF THEOREM 5

First, if we let total travel delay be $T' = \sum_{e \in p^*(\lambda_L)} t_e^*(\lambda_L) > T$, we get a relaxed version of PASO. According to Theorem 4, we know that LB $= \sum_{e \in p^*(\lambda_L)} c_e(t_e^*(\lambda_L))$ is the optimal solution of the relaxed version, and thus we have LB $\leq$ OPT.

Second, since $\sum_{e \in p^*(\lambda_U)} t_e^*(\lambda_U) < T$, we know that $p^*(\lambda_U)$ and $\{t_e^*(\lambda_U) : e \in p^*(\lambda_U)\}$ is a feasible solution to PASO. Thus, $\mathsf{UB} = \sum_{e \in p^*(\lambda_L)} c_e(t_e^*(\lambda_U)) \geq \mathsf{OPT}$.

The proof is completed.